Reactive Structural Materials: Preparation and Characterization

*Daniel L. Hastings and Edward L. Dreizin**

Reactive structural materials, which can serve both as structural elements as well as a source of chemical energy released upon initiation have emerged as an important class of metal-based composites for use in various energetic systems. Such materials rely on a variety of exothermic reactions, from oxidation to formation of metal-metalloid and intermetallic phases. The rates of these reactions are as important as the energy that may be released, in order for them to occur at the time scales compatible with the requirements of applications. Therefore, chemical composition, scale at which reactive components are mixed, and the structure and morphology of materials are important and can be controlled by the method of preparation and compaction of the composite materials. Methods of preparation of the composite structures are briefly reviewed as well as methods of characterization of their mechanical and energetic properties. In addition to common thermo-analytical and static mechanical property measurements, dynamic tests of mechanical properties as well as ignition and combustion experiments are necessary to understand the fragmentation, initiation, and heat release expected for these materials when they are stimulated by an impact, shock, or rapid heating. Reaction mechanisms are studied presently for the thin layers and small samples of reactive materials initiated in carefully designed experiments. In other experiments, impact and explosive initiation are characterized for larger material compacts in the conditions imitating practical scenarios. Examples of results describing thermal, impact, and explosive initiation of some of the reactive materials are presented.

1. Introduction

Reactive Structural Materials (RSMs) are a relatively new group of materials designed to have structural strength and store energy to be released at a desired time.[1–7] Their typical applications are expected in such systems as kinetic penetrators,[8] reactive fragments,[9–11] reactive bullets,[12] reactive armor,[13,14] and munition casings.[15,16] Considering that most structural components in various munitions are based on steel, the utility of RSMs can be semi-quantitatively assessed from a diagram shown in **Figure 1**. The horizontal axis shows a mass fraction of a munition taken by an explosive charge. It is assumed, for simplicity, that the charge is TNT (trinitrotoluene) with the rest of the munition comprised of a metal casing, made of either steel or aluminum. Upon initiation, the case is assumed to oxidize releasing heat in addition to the heat generated by the TNT charge. The percentages of heat released by both TNT and case oxidation are shown for hypothetical scenarios with cases made of steel or aluminum. The estimate shows that for the common mass percentage of the explosive charge, around 30%, the heat release due to the combustion of the metal case can add from ca. 40 to 70% of the total chemical energy produced by the munition. For the common, chemically inert cases, this energy is not released. Thus, releasing even a portion of the total oxidation energy generated by the reacting case could substantially increase the total energy yield of the system.

To maximize this additional heat release due to the metal case combustion, RSMs are typically based on metals with high heats of oxidation, such as aluminum, magnesium, zirconium, and titanium. Alloys based on depleted uranium[17,18] are also considered, in particular for kinetic penetrators, where both high density and high reactivity are important. However, because of radioactivity of uranium, its use in contemporary munitions systems is discouraged.

Perhaps, the first reactive materials reported in literature were composites of aluminum and polytetrafluoroethylene (PTFE, also commonly referred to as Teflon®).[19,20] Although low density and strength of Al-PTFE composites severely limits their applications, such materials were studied rather extensively, representing a common reference system for many RSMs developed recently. In addition to metal-fluoropolymers, the types of RSMs described in the literature include thermites, for example,[21–23] reactive intermetallic systems, such as Al–Ni, for example,[24–26] metal-metalloid systems, including B–Ti, B–Zr, for example,[27–30] systems forming metal carbides, for example,[31] and simply composites and alloys combining materials with different desired properties, for example, tungsten with a high density with zirconium or hafnium, metals with a relatively

Dr. E. L. Dreizin, D. L. Hastings
New Jersey Institute of Technology, Newark, New Jersey, USA
E-mail: dreizin@njit.edu
Dr. E. L. Dreizin
Tomsk State University, Tomsk, Russia
The ORCID identification number(s) for the author(s) of this article can be found under https://doi.org/10.1002/adem.201700631.

DOI: 10.1002/adem.201700631

 © 2017 WILEY-VCH Verlag GmbH & Co. KGaA, Weinheim

Daniel Hastings graduated with a BS in Mechanical Engineering and BS in Information Technology at New Jersey Institute of Technology before entering into the Chemical Engineering PhD Program in the Fall of 2015. His present research focuses on the development of energetic composites with military applications.

Edward L. Dreizin received his MS in molecular physics and PhD in applied physics from Odessa State University, Ukraine in 1985 and 1992, respectively. He immigrated to the USA in 1992 and worked as a Research Scientist at AeroChem Research Labs, Princeton, NJ from 1993 till 1999. He joined faculty at New Jersey Institute of Technology in 1999, where he is presently Distinguished Professor and Associate Chair for Graduate Studies in the department of Chemical, Biological, and Pharmaceutical Engineering. He holds a secondary appointment with Tomsk State University, Russa, since 2014. Prof. Dreizin's research is mostly in the areas of reactive materials and metal combustion.

high reactivity.[32–38] Along with the composition, design of composite RSMs and the methods used for their testing vary widely, depending on the intended application, properties of individual components, and capabilities available to the material designers. This review aims to offer an initial guidance to the potential users and researchers entering the field of RSMs. It first discusses thermodynamic foundations of selecting composites suitable for RSMs, and then discusses some requirements and limitations on the reaction rates necessary for RSMs in selected applications. Different methods used to prepare RSMs are then described along with the respective RSM structures and basic properties. An attempt is made to introduce scale of mixing between reactive components as a common parameter that can be used to quantify different RSM structures. The experimental techniques employed to characterize different RSM energetic and mechanical properties are briefly covered and, finally, the present state of the art is summarized in concluding remarks.

2. RSM Compositions Based on the Heat Release and Density

Different types of exothermic reactions can be exploited to design an RSM. The initial selection of materials can be made accounting for their heat of oxidation. Other exothermic reactions, such as those leading to the formation of fluorides, borides, carbides, aluminides, and silicides are also commonly considered. The heats of reactions are readily available, either from such compilations as NIST – JANNAF tables[39] (available online as NIST Chemistry webbook), summary by Fischer and Grubelich,[40] and other sources. An overview shown in **Figure 2** was prepared using, in addition to the above databases, data from refs.[41–44] It presents heats of reaction normalized per gram and per cubic centimeter of metal fuels for formation of fluorides, oxides, borides, and carbides. Other reactions that have been exploited for RSM produce silicides, sulfides, and aluminides. Two trends apparent in Figure 2 are that reactions of fluorination and oxidation are substantially more exothermic than any other reactions and that, in general, metals with lower densities have greater gravimetric heats of reaction. There appears to be a much weaker difference between different metals when their volumetric heats of reaction are compared to one another. Dashed lines in each plot mark the heat of oxidation for iron, which was used to estimate the percentages of heat release shown in Figure 2. Metals/reactions with close or higher values of heat release are of potential interest in RSM. It thus appears that almost any metal could be attractive for the applications, where the volume needs to be minimized, while

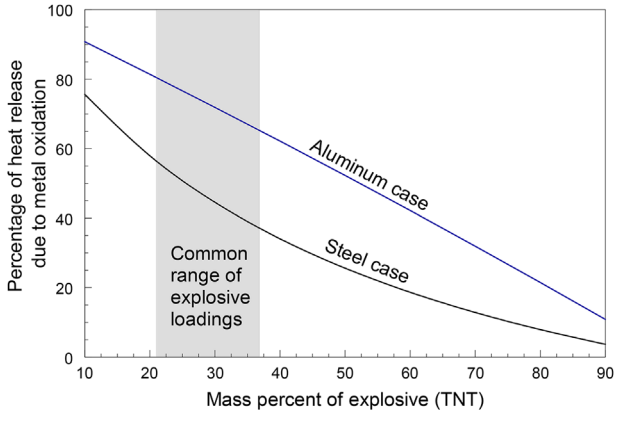

Figure 1. Estimated fraction of heat release due to complete oxidation of a metal case for a hypothetical munition containing varied mass percent of TNT as an explosive.

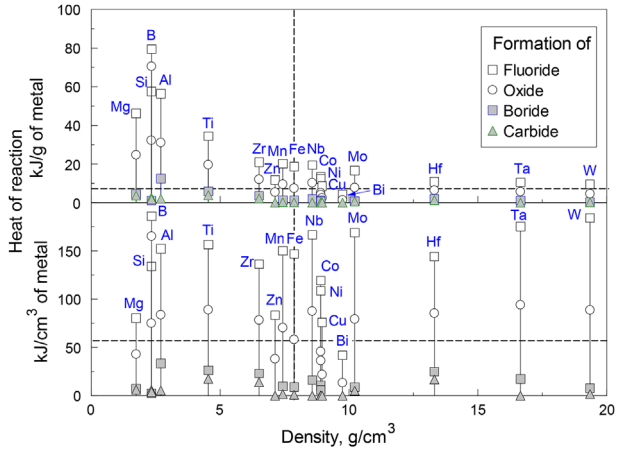

Figure 2. Gravimetric and volumetric heats of reaction for selected metals as functions of the metal densities.

© 2017 WILEY-VCH Verlag GmbH & Co. KGaA, Weinheim

greater mass is acceptable. In particular, volumetric heats of oxidation of relatively high-density metals, such as Mo, Nb, Hf, Ta, and W are greater than those of iron. Therefore, it could be possible to extract from RSMs energies greater than shown in Figure 1 for the munitions, in which steel cases are replaced with reactive materials based on the above metals. Of course, reaction enthalpies, such as shown in Figure 2, offer only the initial assessment, while the ability to reach the rate of heat release necessary to make the exothermicity useful is another important consideration that needs to be accounted for while designing RSMs.

3. Rates of Heat Release for RSMs

Taking full advantage of the heat of oxidation or other reactions involving material components used in RSMs is difficult; it requires heterogeneous reactions with fast kinetics and breaking of the structural parts into fine fragments, which can burn in time scales defined by the specific application. Each specific application defines its own range of the acceptable time scales; these scales range from minutes, in the case of signal flares,[45] to milliseconds for blast charges,[46] or down to microseconds for kinetic penetrators.[47] Some specific examples are considered here to illustrate an approach guiding the designs of RSMs for specific time scale requirements.

The shortest reaction time scales are necessary for armor piercing projectiles, which impact targets at speeds in the range of 1800–2900 m s^{-1}.[47] Assuming the penetration depth $d \approx 100$ mm, the time for the reaction to occur for the chemical energy to be coupled with the kinetic energy of the impact, can be estimated as, $t \approx d/v$. Thus, the timescales are on the order 35–55 μs. These times are shorter than any reported times of combustion for metal particles or nanoparticles in gaseous oxidizers; besides, the gaseous oxidizers may not be readily available in many practical scenarios, for example, involving impacts in upper atmospheric layers or underwater. Thus, the reaction for such applications must occur between the components of RSM; it would occur heterogeneously and be rate controlled by mass transport of the reactive components toward each other. To crudely estimate appropriate reaction rates, consider characteristic diffusion coefficients in various metal oxide and intermetallic phases, which range typically from 10^{-10} to 10^{-3} cm^2 s^{-1}.[48–51] Note, however, that the diffusion coefficient is a strong function of temperature; it can also change dramatically for different diffusion mechanisms.[52] For example, diffusion coefficients as high as 10^{-8} cm^2 s^{-1} are reported for the grain boundary diffusion in alumina,[53] a common product of thermite reaction. The diffusion coefficient, D, can be used to estimate the characteristic reaction time as $t = L^2/D$, where L is the diffusion length. The diffusion length may be evaluated as the scale of mixing between the reacting components, and plugging in the characteristic diffusion coefficients and times above, the range of mixing estimated varies from 0.02 to 7.5 nm. Clearly, the lower bound, obtained using $D = 10^{-13}$ cm^2 s^{-1} is not physical; however, the upper bound approaching 10 nm and relying on the rapid, grain boundary diffusion is achievable for the materials mixed on the nanoscale and having multiple defects and grain boundaries in the layers separating reactive components. The same estimate suggests that coarser scales of mixing, ca. 30 nm and above may be useful when the characteristic reaction times exceed 1 ms.

For applications where external oxidizer is available, initial heterogeneous reactions may only be needed to ignite RSM fragments; the continued combustion of such fragments may occur at much longer time scales, for example 10–50 ms.[46] In such cases, the reaction may occur either on the surface of the produced fragments or in the vapor phase and be primarily controlled by the fragment sizes. Clearly, the rates of combustion will depend on the oxidizing environment and pressure, flow conditions, and fragment materials. For the initial guidance in selecting the appropriate fragment size, one can consider burn times of typical metal particles reported in the literature. A summary of such data is shown in **Figure 3**. Because a comprehensive summary of many published datasets for different metals cannot be clearly represented in a single plot, only selected results are shown. For each metal, the burn times are shown for two ranges of particle sizes, representing coarser and finer powders. For each range of particle sizes, a descriptive trend expressing the burn time proportional to the particle size in the power n is shown as a dashed line, with the symbols representing the ends of the respective particle size ranges. Some of the trends shown are based on more than one set of measurements reported in the literature. The data for aluminum come from refs.[54,55] for boron, from refs.[56–58] for titanium, from refs.[59–61] and for magnesium, from refs.[62–65] It is apparent that there are discrepancies between the trends for coarse and fine particles for all metals, which is likely associated with errors in measurements. Despite the errors, the trends shown can be used for the initial assessment of the burn times for the fragments with the specified dimensions. It is observed that for all particle sizes, boron particles have the longest burn times, while the shortest burn times are reported for particles of magnesium. Burn times for the same size aluminum and titanium particles are very close to each other. The data summarized in Figure 3 suggest that magnesium particles as coarse as 200–300 μm diameter can still be useful if the reaction times can be extended to 50 ms. However, the particle sizes for

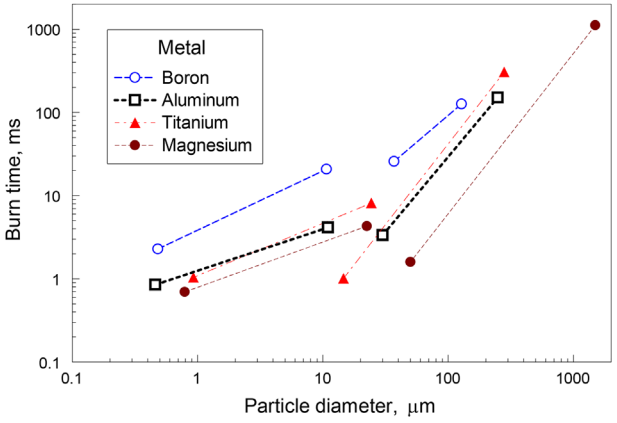

Figure 3. Characteristic burn times of particles of different sizes for selected metal fuels reported in the literature: aluminum,[54,55] boron,[56–58] titanium,[59–61] and magnesium.[62–65]

© 2017 WILEY-VCH Verlag GmbH & Co. KGaA, Weinheim

boron must be finer than ca. 50 μm in order for them to react in the same time.

4. Structures of RSM and Methods of Their Preparation

4.1. Reinforced Composites with Micron- and Coarser Components

Composites combining aluminum powder with PTFE were proposed as RSMs more than a decade ago,[66] probably building on the well-known Mg/PTFE composites used in pyrotechnics. The most common composition is the stoichiometric mixture comprising 26.5 wt% of Al and 73.5 wt% of PTFE. Typically, such composites are prepared by blending powders of Al and PTFE and consolidating them by uniaxial or isostatic compression. An elevated temperature, typically between 375 and 385 °C, is used during consolidation to ensure the structural integrity.[67] The methodology is refined in further work, for example, refs.[68–70] The materials can be pressed to more than 99% of their theoretical maximum density (TMD), which is approximately 2.33 g cm^{-3} for the stoichiometric composition. PTFE is a very attractive oxidizer thermodynamically, and the interest in metal-PTFE composites as RSM has been maintained over the years. More recently, composites incorporating other metals, such as titanium, zirconium, tungsten, and others in addition to, or instead of aluminum were prepared and characterized.[70–74]

Composites prepared as consolidated blends of metal powders have substantially higher densities, but are less reactive than Al/PTFE. Perhaps the most studied composition is based on nickel and aluminum with the TMD of 6.95 g cm^{-3} for the stoichiometric composition containing 31.5 wt% of Al and 68.5 wt% of Ni. The composites were prepared by cold pressing, with densities in the mid to low of 90% of TMD,[75] radial forging,[76] and by cold spray, although the powders were ball-milled prior to spraying.[26] A combination of hot isostatic pressing (HIP) with monitoring heat release in the consolidated sample[77] was used to prepare low-porosity, RSM components, while retaining their micro-structure and reactivity in the consolidated shapes. The cold spray may also be interesting as a technique enabling consolidation of RSMs from powders without substantial heating necessary and leading to a relatively high product density.[78] It was also applied to consolidate Al–CuO thermite.[21] Other reactive composite systems were prepared by hot pressing elemental powders, for example, W–Zr.[32]

More recently, control of fragmentation of the RSM was attempted by varying the particle size[72] and, even more interestingly, structure of the composite material, which can be changed replacing a powder with fibers.[79] Composites with tungsten fibers embedded in aluminum were prepared using a combination of cold isostatic pressing (CIP) and HIP, which could be followed by an additional heat treatment to harden the aluminum matrix.[80] Prepared materials contained mesostructures including tungsten fibers embedded in aluminum while being placed strategically in both hoop and axial directions, as shown in **Figure 4**.[81] When loaded dynamically, the structure fails when tungsten fibers oriented in the axial direction buckle,

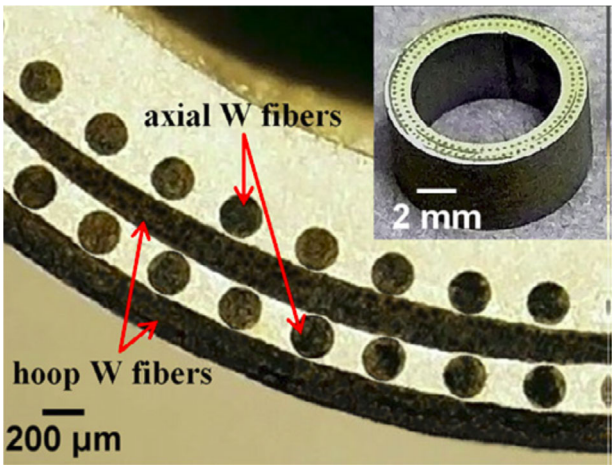

Figure 4. Composite reactive materials with tungsten fibers embedded in aluminum matrix. Microstructure Al-composite tube (see inset) with W fibers in hoop and axial directions.[81]

which is facilitated by the initial fracture of the circumferential fibers.[81] Thus, materials with mesostructures offer additional capabilities for the pre-programmed break up upon its shock loading.

4.2. Composites with Nano-Sized Components

Availability of metal nanopowders led to significant research efforts dedicated to preparation and testing structures with nanoparticles replacing regular metal particles in composites. Following up on the work with coarser powders, Al-PTFE composites were prepared and characterized using nano-powders of aluminum.[82–84] The focus has been on reaction mechanisms and rates rather than mechanical and structural properties of such composites. Substantial efforts were also dedicated to preparing and characterizing various nano-thermite type materials starting with the nanopowders of metal fuels and oxidizers. The powder mixing is commonly achieved via ultrasonication of the starting components.[85] The products are commonly loose powders, which are difficult to consolidate as necessary for most RSM applications. However, ultrasonic vibrations, similar to those used in ultrasonic welding, have been successfully used to consolidate samples of nickel–aluminum[86] and nano-thermites with binary and more complex, for example, Al–Ni–CuO and Al–Ni–Fe_2O_3 composites.[87,88] Other methods, including sol-gel chemistry[89–92] and self-assembly[93–96] were used to prepare nano-composite thermites; typically the products are highly porous and may include additional components, such as chemicals used to functionalize metal surface, resulting in a reduced energy density. Continuous, uniform, and flexible laminate structures containing a nanothermite with a polymer binder was recently prepared by electro-spray deposition.[97] A good review of different types of reactive nanocomposites is available in Ref [98].

Recently, additive manufacturing approaches have been explored to generate controlled architectures of RMs, for which burn rate and gas generation can be tuned while using the same

© 2017 WILEY-VCH Verlag GmbH & Co. KGaA, Weinheim

nanocomposite thermite.[99,100] Nanothermite structures comprising micro-channels and hurdles were created starting from nanopowders of Al and CuO. Compared to a non-patterned material, the flame propagation velocity was tripled and halved for channels and hurdles, respectively.

While significant progress has been made preparing various shapes and morphologies of RMs using nanoparticles of starting materials, most of the prepared continuous structures were limited to relatively thin, quasi two-dimensional layers; three-dimensional items prepared were typically very porous and had low strength, limiting their applications in RSMs.

4.3. Layered and Nano-Layered Systems

Fully dense composites suitable for RSM applications have been prepared by mechanical processing bulk metals or packed powders using swaging, a cold forging process reducing diameter of tubes.[76,101] The scale of mixing achieved in such a processing and the structure of the layered system are illustrated in **Figure 5** for a composite prepared from nickel flakes with powders of aluminum and magnesium. The mixing scale achieved is rather coarse, with the thickness of about 1 μm for the finest Ni layers. Minor porosity is also observed, although most of the sample is fully packed. Based on density measurements, the volume fraction of voids was estimated to be within 0–5%.

A variety of RMs were prepared as nanolayered systems, using vacuum deposition based techniques.[102] The structure of such materials can be precisely controlled and the layer thickness can be as small as 10 nm. Earlier work focused on intermetallic systems, such as Al–Zr, Ni–Al, and others[103–106]; more recently, significant progress has been made preparing various thermite-type materials.[107–111] RMs with planar, well-defined layers of individual composites and with essentially no porosity serve as a convenient model material for studies of reaction mechanisms. Varying the thickness of the deposited layers enables one to manipulate directly the mixing scale between the components. It has been recognized, however, that poorly defined phases exist at the interfaces between the reactive components deposited on top of each other by sputtering. To avoid uncontrollable formation of the intermediate reaction products, additional layers were formed between the reactive components by atomic layer deposition.[112–114] Such layers, although still serving as diffusion barriers, can be better controlled, leading to a more predictable behavior of the RM system. An example of such a custom-engineered RM is shown in **Figure 6**. Although the added intermediate phases create diffusion barriers between the reactants, slowing down the rate of heat release, this effect may be tuned by adjusting the thickness and type of the added interfacial layers.

Various approaches were explored for preparing optimized layered systems; for example, the order in which the metal and oxidizer are layered, and which material ends up on the surface, can affect how the material ages over time. Depositing aluminum or magnesium onto preliminarily grown, ordered nano-columns of an oxide (e.g., CuO or Co_3O_4) leads to interesting morphologies, for which the reaction rate is different than for a planar layered system.[115,116] Further, such systems can be modified by added layers of fluorocarbon,[117,118] making the surface of the prepared material hydrophobic.

4.4. Mechanochemically Prepared or Mechanoactivated Materials

Composite powders were prepared mechanically milling starting components, present as micron-sized particles, flakes, or even bulk pieces.[119,120] This technique, developed initially for preparation of mechanically alloyed and dispersion strengthened composites,[121,122] was extended to process materials of interest to RSMs. Such materials include reactive metals and intermetallic systems, such as aluminum, magnesium, nickel, zirconium, titanium, etc., and composites, including all types of chemistries discussed above, as well as metals with even more aggressive oxidizers, such as $KClO_4$, NH_4ClO_4, etc.[123] Mechanical milling typically yields powders with particle sizes in the order of 1–100 μm. Each powder particle is a nearly fully dense composite. The components are mixed within such particles on the scale of ca. 100 nm. The interfaces formed in mechanochemically prepared particles form because of interaction between the components during milling. Such interactions mostly involve mechanically induced shear accompanied by pressing the components together by colliding milling media. These interactions occur at the milling temperature, which is typically just slightly higher than the room temperature. Thus, the components are rather inert chemically, so that the interfacial layers

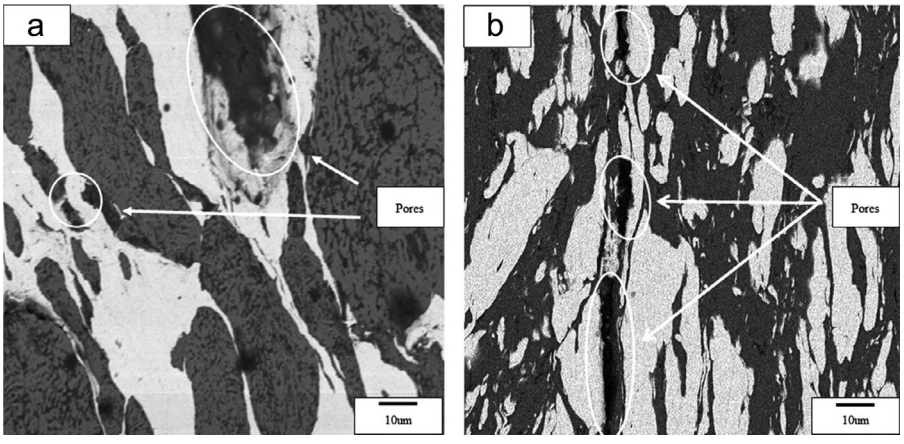

Figure 5. Microstructures of the composite prepared by swaging using powders of Al and Mg with flakes of Ni. Minor porosity is observed. Most of pores appear between Ni flakes and at boundaries between Ni and Al.[76]

© 2017 WILEY-VCH Verlag GmbH & Co. KGaA, Weinheim

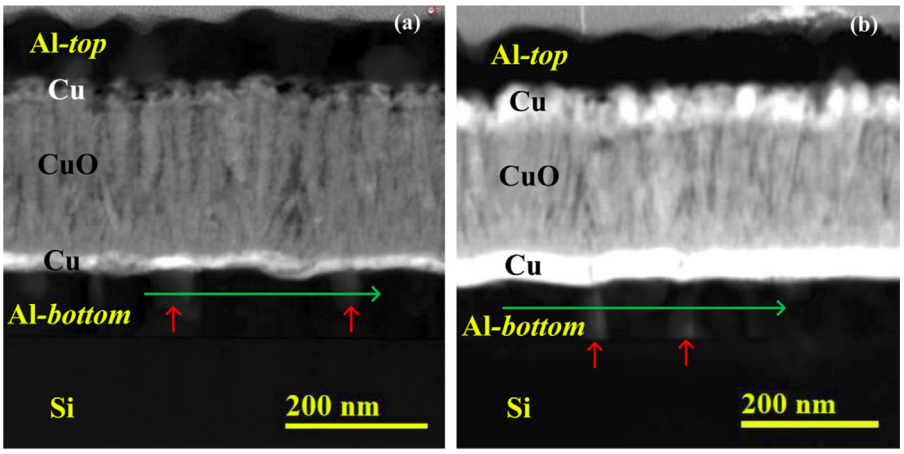

Figure 6. High-angle annular dark-field scanning transmission electron microscopy images of Al–CuO nanocomposites prepared by magnetron sputtering and including 41 wt% Cu a) and 63 wt% of Cu b) between Al and CuO layers.[113]

produced may be thinner than for the composites prepared by vacuum deposition or than surface oxide layers, such as amorphous alumina, always present on the metal particles exposed to an oxidizing environment. Using such powders for preparing RSMs has its advantages and drawbacks. The advantages are the relatively coarse particle size, combined with the fine mixing scale for the reactive composites, making handling such powders easier than that of the nanopowders with the same or comparable scale of mixing. It is also important for the mixing scale and morphology to be preserved while the powder is being handled. However, mechanochemically prepared powders are typically work hardened (or less ductile), making it more difficult to consolidate them into bulk items.

Consolidated shapes were readily prepared using mechanochemically prepared metal-fluoropolymer composites by slightly pressing them.[124,125] These highly energetic materials have relatively low density and strength. Fuel-rich thermites were consolidated by uniaxial pressing, achieving densities close to 90% of TMD without binders.[126] Added binders, either polymers or low-melting metals improved mechanical properties, but reduced the energy density of the consolidated composites.

5. Characterization of RSMs

5.1. Mechanical Properties

As for any structural materials, mechanical properties are of critical importance for RSMs. Static mechanical properties, such as tensile, yield, compressive, or flexural strength are routinely measured using standard tests.[127] However, in many cases, prepared RSMs may not be available in the form of specimen required for the most common standardized tensile yield test; sometime preparing such specimen is problematic because the composites are brittle. In such cases, often compressive strength of RSMs is measured instead using so-called Brazilian test, in which a disk-like specimen is compressed with a continuously increasing load until it fails.[128] Static tests, while important, are not specific for RSMs and will not be discussed here in further detail.

Dynamic mechanical properties of RSMs are measured using Split Hopkinson Pressure Bar (SHPB).[129] SHPB is probably the most common test enabling one to characterize dynamic response of a material. The achievable strain rates vary from 50 to 10^4 s^{-1}. The experimental setup is shown schematically in **Figure 7**.[130] The sample or specimen is placed between input and output bars. The input bar is loaded by a striker bar, which can be accelerated using a gas gun. An incident pulse (or stress wave) propagates through the input bar toward the specimen where it splits into transmitted and reflected pulses. The transmitted pulse may deform the sample plastically. Thus, it can be substantially changed as it travels through the sample and into the output bar. The reflected pulse travels back down the input bar. There are strain gauges in both input and output bars, which measure strains caused by the traveling waves; an analytical model is used to process the output of the strain gauge readings and recover mechanical properties of the material. Additional optical measurements can be used to detect an exothermic reaction initiated in an RM sample by the impact.

Multiple examples of the SHPB-based experiments characterizing RSMs were reported in the literature, such as.[33,81,131–135] For example, Al-PTFE composite materials were found to be sensitive to the strain rate; it was further reported that the compressive strength is maximized at the aluminum fraction of 35 wt%.[132,134]

An example of a sequence of high-speed video frames taken during an SHPB experiment with a hot pressed RSM comprising 33 wt % of W and 66 wt% of Zr is shown in **Figure 8**.[33] Processing the recorded video along with the analysis of the incident, transmitted, and reflected pulses recorded by strain gauges enabled researchers to determine that the dynamically measured compressive strength of the sample was higher than that measured in static tests. It was also observed that the specimen failed at only about 2% of strain, behaving as a typical brittle material. Different type fragments formed upon the sample failure and exhibited different combustion regimes, identified from the video.

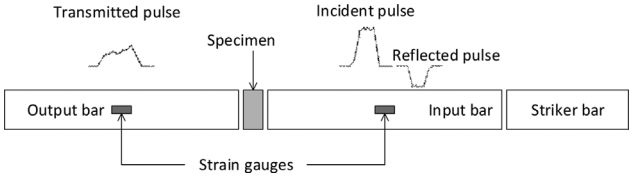

Figure 7. Schematic of the SHPB, following ref.[130]

© 2017 WILEY-VCH Verlag GmbH & Co. KGaA, Weinheim

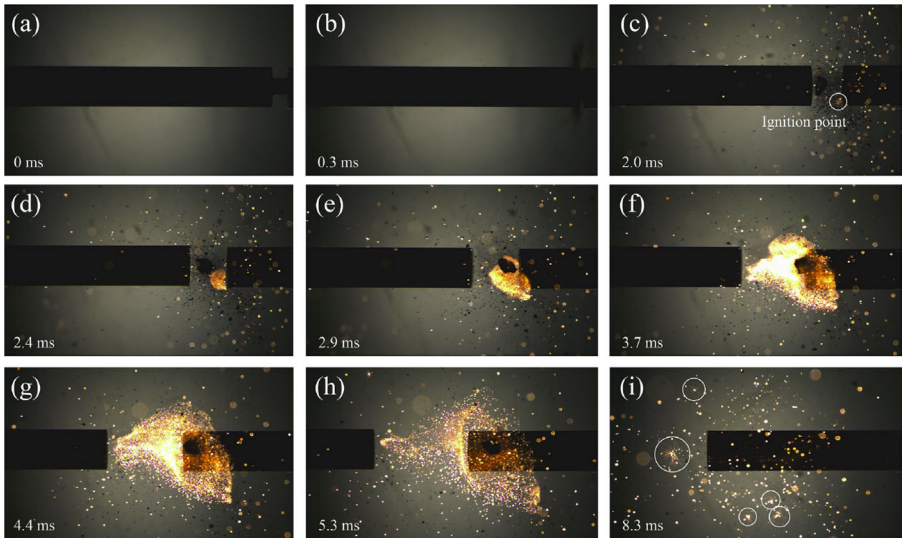

Figure 8. Selected frames from a high-speed video record of ignition and propagation of a Zr–W samples in a SHPB test at 23.53 m s^{-1}. A record rate of 30000 frames s^{-1} and shutter speed of 1/40000 s were used. The timestamp of each frame is measured from the start of deformation.[33]

Other dynamic tests include Taylor impact, in which a cylindrical projectile made of the material being tested impacts onto a large flat plate, or anvil.[136] The impact velocities a round 100–200 m s^{-1} cause a non-uniform deformation of the projectile. Strain rates exceed 10^5 s^{-1}, and thus are higher than those in the SHPB test. A model is available that correlates the residual geometry of the deformed projectile with the dynamic yield strength. A more detailed modeling involving state of the art hydrocodes, such as CTH,[137,138] are also used to interpret such tests for RMs.[25] High-speed videos are used to detect the ignition and record changes in the sample shape while it is being deformed. Such videos help recovering dynamic values of the yield stress during the test; such measurements are particularly valuable if the sample ignites and thus changes its shape before being recovered. Results of Taylor tests showed that a cold-sprayed Ni–Al composite is more reactive than the same composite consolidated by explosive compaction.[25] Sometime, a reverse Taylor test is performed, in which the RM cylinder is stationary and the projectile serves as the anvil.[139] Modifications of this test are also being developed using instrumented plates, high-speed video, and post-mortem analysis of the compacted and initiated samples.[140,141]

5.2. Thermal Analysis

Thermal analysis has become the most common and versatile technique for studying thermally activated chemical reactions, which are of critical importance to RSMs. Aging of such materials is certainly governed by the reactions occurring both at their surfaces, interacting with the environment, and at the internal interfaces between reactive components. It can also be argued that the thermally activated reactions are critical for ignition of RSMs even when the practical ignition stimuli are the shock or impact. In those cases, multiple models have been developed to predict formation of so-called hot spots, caused by various defects and irregularities in the loaded structures.[142–148] Once such defects are developed, they self-heat, leading to ignition, which then can be described as a developing thermally activated reaction. Thus, the importance of thermo-analytical measurements, including thermo-gravimetry (TG) and differential scanning calorimetry (DSC) cannot be overestimated. Not surprisingly, most researchers developing RSMs or relevant compositions have applied DSC and TG to characterize their materials. A review describing relevance of such measurements to ignition mechanisms of aluminum-based RMs is available.[149] Ideas discussed there are also applicable to other types of RMs.

Measurements performed at different heating rates are routinely used to establish kinetics of various reactions. Various isoconversion processing techniques are used; recently, useful recommendations for the data processing were proposed, which are fully applicable for studies of RSMs.[150] Similarly, recommendations are available for collecting the thermo-analytical data.[151]

Without reviewing a very extensive set of references, where thermo-analytical measurements were used to characterize various RSMs and relevant structure, one overarching observation can be made coming from the authors own studies.[119,120,152] While multi-step exothermic reactions are commonly observed in DSC traces, it is most commonly the very first, low-temperature reaction step that governs the ignition behavior of the material, when it is heated rapidly. This initial step may not necessarily be the strongest among different reactions observed. However, accounting for it becomes critically important when one attempts interpreting ignition of both thermites and intermetallic-based RM composites.

New experimental methods, expanding the capabilities of conventional thermo-analytical measurements take advantage of miniaturized heating elements, which can achieve heating rates exceeding 10^4 K s^{-1}, approaching those expected in the RSM ignition scenarios.[153] Such measurements, limited to very small samples and affected by possible temperature gradients in the heated material are useful to bridge the understanding of reaction mechanisms obtained from DSC with the processes occurring in ignition, as discussed below.

5.3. Ignition and Combustion

5.3.1. Ignition Experiments

Ignition and combustion measurements are performed for both consolidated RSMs and for powders used to prepare RSMs. It is commonly assumed that if an RSM fragments upon initiation, ignition and combustion of the produced fragments

© 2017 WILEY-VCH Verlag GmbH & Co. KGaA, Weinheim

is reasonably well represented in studies dealing with the powder particles.

Ignition of small amounts of RM powders is commonly studied using an electrically heated metal filament with a thin deposit of an RM powder.[154] The filament temperature may be monitored using an infrared pyrometer, or it can be obtained from the filament's resistance, calculated using the measured current and voltage.[155,156] The ignition instant is detected optically and the measured temperature of the filament is treated as the ignition temperature. The heating rate may be varied to observe a shift in the ignition temperature, suitable for quantifying the respective reaction activation energy. Depending on the filament diameter and the power supply, the heating rates attainable are from 100 to 10^6 K s^{-1}. This method was used extensively to determine how the ignition temperature changes as a function of the heating rate for a broad range of RMs prepared by mechanical milling, for example,[157–162] as well as for other types of RMs.[163–166] In a variant of this experiment, the powder-coated wire is mounted in a vacuum chamber connected to the inlet of a time of flight mass spectrometer (TOF-MS).[156,167–170] Thus, release of gaseous species emitted by the heated and ignited RM is described in real time. A characteristic result is illustrated in **Figure 9**, where the RM sample is prepared by vacuum layer deposition of Al and CuO nanolayers directly onto a platinum filament.[163] The vertical dashed line indicates ignition observed in a high speed video. An oxygen peak occurs before ignition, whereas onsets of peaks of Al, Al_2O, and Cu coincide with the ignition instant. The early oxygen release was proposed to be associated with decomposition of the heated CuO, which was confirmed by separate experiments.[171] A similar behavior was observed for nanothermites with several other oxides used as oxidizers. A qualitatively similar oxide decomposition was observed to precede ignition for fully-dense thermites prepared by mechanical milling, although the experiments were not performed in a high vacuum so that no CuO decomposition was detected without the presence of Al. It was proposed that for the milled materials, pre-ignition heterogeneous reaction between Al and CuO partially reduces CuO prior to ignition, yielding a metastable CuO_{1-x} phase (1>x>0), which decomposes upon heating.[160]

An idea of correlating the ignition with intermetallic exothermic reactions in an RM, discussed in detail in ref.[149] is illustrated in **Figure 10**.[162] For comparison, the positions of exothermic peaks from thermo-analytical measurements and ignition temperatures obtained from the heated filament experiments are plotted in the same Arrhenius coordinates for the same mechanically alloyed Al · Ti powders. The peaks in DSC traces were assigned to a weakly exothermic intermetallic reaction producing $L1_2$ phase of Al_3Ti. The results of the ignition experiments correlate well with the trend-line for the DSC measurements. Extrapolating this trend-line to even higher heating rates enables one to predict an ignition temperature (shown by filled black symbols) in more practical scenarios.

Other techniques used for thermal initiation of RMs include use of laser heating for individual particles[172,173] and for pressed bulk samples.[149,174] Heating rates approaching 1 0^6 K s^{-1} are achieved. If used for the same materials, ignition temperatures observed in the laser heating experiments can be compared to those expected from the kinetic trends obtained

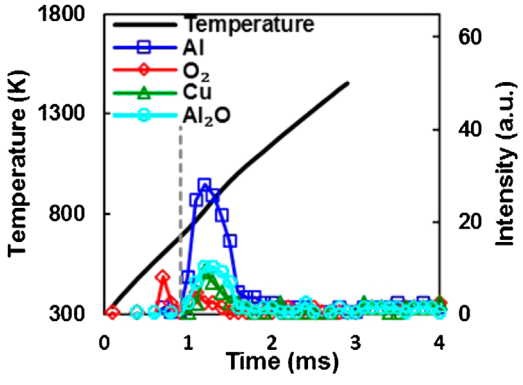

Figure 9. TOF-MS results from experiments for a reactive Al–CuO nanofoil prepared by vacuum deposition with six bilayers.[163]

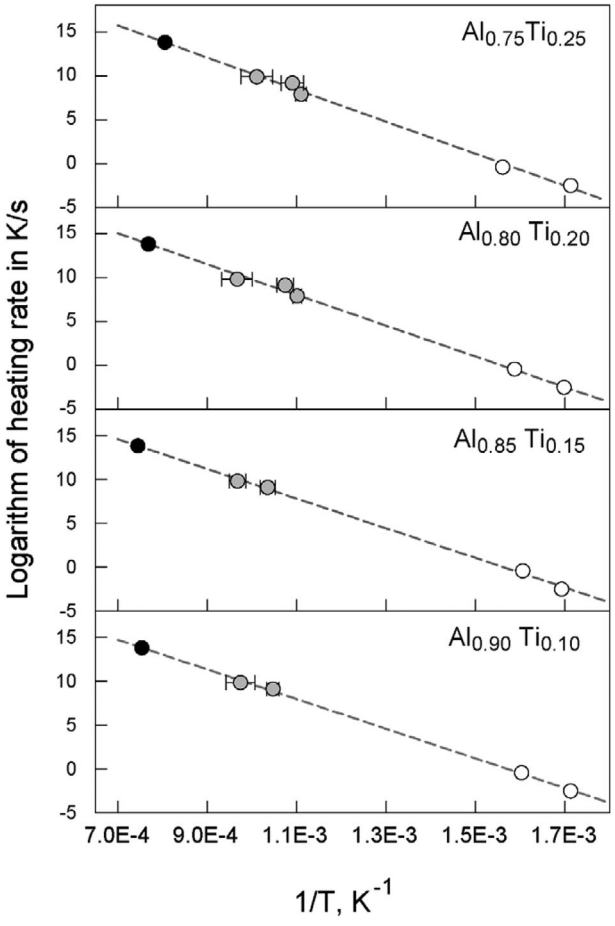

Figure 10. Arrhenius plots combining different measurements for mechanically alloyed Al Ti powders. Results of thermo-analytical measurements representing formation of $L1_2$ phase of Al_3Ti are shown as open circles. Ignition temperatures measured using the electrically heated filament shown as gray circles. Ignition temperatures, estimated for the heating rate 10^6 K s^{-1} expected in the laminar lifted flame experiments are shown as black circles.[162]

© 2017 WILEY-VCH Verlag GmbH & Co. KGaA, Weinheim

from thermal analysis and/or from the heated filament experiments. Still higher heating rates, in the range of 10^9 K s^{-1} are achievable in the experiments using an electrostatic discharge (spark) as an ignition source.[175–178] An increase in the heating rate can cause a qualitative change in how the reaction propagates.[179] At very high heating rates, substantial temperature gradients develop across RM domains. This can cause localized reactions to occur while the rest of the material is being heated and/or melts. Thus, the fine structure of the composite material may be preserved to much higher temperatures and through greater reaction progress than anticipated for low-heating rate events, in which melting of the material components results in a loss of the initial structure and scale of mixing.

A methodology for studying shock initiation of thin RM layers using a very short laser pulse was developed.[180–184] A picosecond laser flash heating vaporized the surface of an RM target. The RM, typically a nano-aluminum/reactive binder composite, reacts involving surrounding oxidizing environment. A spherical shock wave is generated while its pressure drops rapidly. The shock decomposes the binder (nitrocellulose or Teflon®) down to a characteristic diameter of reaction. That diameter was measured as a function of the laser energy. A hydrodynamic model was developed to interpret results; the model assumed that chemical reactions occur when a threshold pressure applied for a given time duration. A similar technique was recently used to study shock initiation of RM samples based on porous Si.[185]

Microscopic samples of various RMs were impact initiated in recent experiments using metal foil-based flyer plates.[178,183,184,186–188] In a typical experiment, illustrated in **Figure 11**, a thin copper foil is used as a flyer plate; aluminum foils were also used. The foil is initially epoxied to a glass and is accelerated by a pulse from an Nd:YAG laser. The impact produces a planar shock in the target material, in this case, an Al-PTFE nanocomposite. The speed of the flyer can exceed several km s^{-1}. The shock duration is varied around 10 ns; it depends on the material impacted by the flyer. Prior to the launch of the foil, the target material is placed at the impact location using an optical microscope. High-speed optical probes track emission, and, in the most recent experimental development, spectra emitted by the impact-initiated target material with ps resolution.[188,189] Time-resolved details of shock-compression initiation can be detected, which are not currently accessible by any other techniques. These experiments serve to establish mechanisms of shock initiation, hot spot formation, etc. However, because the flyer plate typically quenches the initiated reaction, the reaction at longer time scales may not compare well with that expected in a practical configuration.

A new generation of measurements of initiation mechanisms in RSMs take advantage of the advanced analytical techniques, such as dynamic transmission electron microscopy (DTEM)[190,191] or time-resolved X-ray diffraction studies enabled by high-intensity X-ray beams produced by synchrotron radiation.[192] Such measurements enable direct observation of changes in morphology and structure of the RM particles initiated directly under the microscope or in the diffractometer. It was observed, for example, that for the thermites prepared as mixed nanopowders, condensed phase and interfacial reactions, as opposed to gas release, are fast enough to serve as dominant combustion mechanisms.[190]

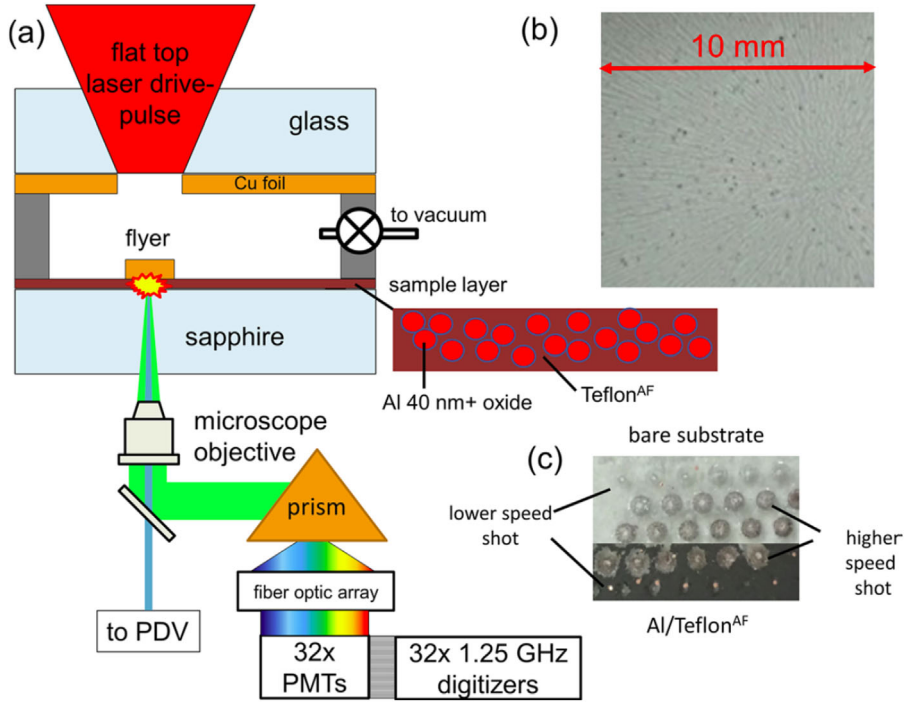

Figure 11. a) Schematic of the apparatus using laser-launched 25 μm thick Cu flyers to shock a 3 μm thick film of Al/Teflon. b) Optical micrograph of Al/Teflon film on sapphire. c) A sample after the experiment. Prior the experiment, a portion of the Al/Teflon film is scraped away to yield a bare region which was used to precisely calibrate flyer velocity versus launch laser energy. The darker region with Al/Teflon shows reacted regions for lower speed (0.7 km s^{-1}) and higher-speed (1.5 km s^{-1}) shots. The reaction produced with the higher-speed shots extends several mm beyond the 0.5-mm diameter flyer. The impact areas are 4 mm from one another.[188]

5.3.2. Combustion of RM Particles and Particle Clouds

These experiments follow, generally, the same methods as used to study combustion of individual metal particles or powder clouds. Particles are ignited, typically by a laser beam[173,193] or while being injected in a flame[194–197]; their combustion times and temperatures are measured based on their optical emission. Different methods were used to correlate the particle sizes and their combustion times. Recently, such correlations were obtained by comparing the measured statistical distributions

© 2017 WILEY-VCH Verlag GmbH & Co. KGaA, Weinheim

of particle sizes and their burn times.[173] In that processing, larger particles are assumed to burn longer than smaller ones. it is assumed that larger particles burn longer.

Results with multiple RM particles ignited in a reflected shock wave were also reported.[198,199]. In such experiments, the burn times are usually obtained measuring the width of the optical emission pulse. The obtained burn time is correlated with the average particle size for the powder used in experiments.

In other experiments, typically performed with the RMs comprising mixed nanopowders, combustion of a loosely packed RM sample in an open tube is studied.[200–203] Although most measurements focused on the apparent flame propagation rate, it was understood recently that this rate is superficial and is associated with incandescent particles moving along the tube.[204,205] It was reported that the nanoparticles agglomerate rapidly and form mesoparticles, which burn in the time scales comparable to those for common micron-sized metal particles.

Constant volume explosion experiments are rather common[157,164,173,193,196,206]; they can be performed in vessels of different sizes, with different powders initiated using a heated wire, pyrotechnic igniter, or a spark. Pressure is usually measured in real time and the maximum achieved pressure is associated with the total energy release. The reaction rate is quantified based on the recorded rate of pressure rise. Because not all powder is ignited and because a fraction of the ignited particles is quenched on the vessel walls, the efficiency of combustion may be low. However, this technique is useful for comparing different RM powders to one another. When interpreting these experiments, it is necessary to account for differences in flowability of different powders, which can substantially affect formation of the aerosolized cloud and thus its combustion dynamics.

Examples of luminous streaks produced by Al · Mg alloy particles ignited by a CO_2 laser beam are shown in **Figure 12**.[207] The particles were fed vertically up crossing the laser beam directed horizontally. Once ignited, they burned in ambient air. Labels in each image show the Al/Mg atomic ratios for different samples. The streaks include two bright parts; the first, associated with the selective combustion of Mg followed by the second, produced by predominantly Al combustion.

Pressure traces measured in the constant volume explosion experiments in air for the same mechanically alloyed Al · Mg powders are shown in **Figure 13**.[207] The results show that the maximum pressures are almost the same for all materials and for the pure aluminum. However, the rates of pressure rise are substantially increased for the mechanically alloyed powders.

Burn times measured for several nanocomposite RM powders prepared by mechanical milling and injected in an air-acetylene flame are shown in **Figure 14**.[208,209] These RMs contain such additives as I_2, Cl_2, or S, expected to generate biocidal combustion products aimed to inactivate biological agents, such as anthrax-laced powders. They can be used as liners in the respective munition systems. The results, obtained from a correlation between the measured statistical distributions of particle sizes and burn times are compared to those for pure aluminum and magnesium. It is observed that only one of the prepared materials, Mg · S composite, burned faster than pure Mg (and thus, faster than any other metal, compare to Figure 3). All aluminum-based powders burned slower, than the pure Al.

5.3.3. Impact Initiation of Bulk RSMs

Experiments on impact initiation of bulk RSM samples are often designed to reproduce scenarios expected in the practical applications. For example, it may be important to establish that the material survives launch of a projectile, penetration through a protective layer, and/or capable of coupling the released chemical energy with that of the mechanical impact. It also often desired to characterize the fragmentation of the RSM upon impact and assess the reactivity of the produced fragments.

A very simple experimental testing of the impact sensitivity of reactive composites is possible using a commercial drop weight impact tester, where a pellet is placed on an anvil and hit by a weight falling from a pre-set height.[210] The impact energies may reach several J. Ignition was detected monitoring the infrared emission from the impacted samples. Pellets of several aluminum-based intermetallic composites were pressed and tested. For the relatively low compaction achieved by uniaxial pressing (less than 80% TMD), the results suggested an increased sensitivity to ignition at greater compaction, as illustrated in **Figure 15**. It was also reported that the size of Al particles used in the compacts had only marginal effect on the measured ignition sensitivity, in contrast with laser ignition studies, where the particle size of aluminum affects the ignition temperature of composite RMs substantially. It was proposed that ignition was caused by piercing aluminum particles by harder particles of higher density metals, which broke down the protective alumina shell and exposed aluminum to the external oxidizer.

Variations in the drop weight impact techniques, for example, when a sample is

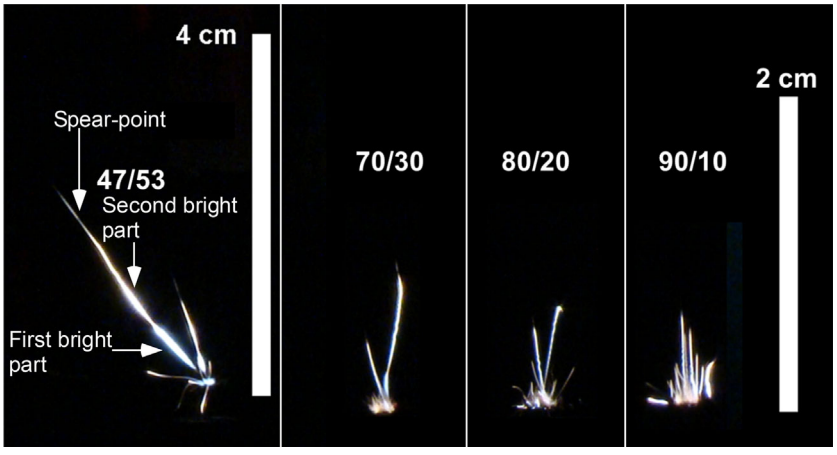

Figure 12. Streaks of burning particles of mechanically alloyed Al · Mg powders ignited by the CO_2 laser beam; scale bar for 70&z.urule;30, 80&z.urule;20, and 90/10 compositions is the same.[207]

© 2017 WILEY-VCH Verlag GmbH & Co. KGaA, Weinheim

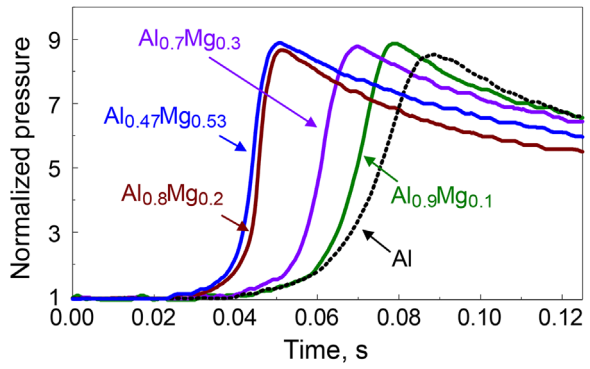

Figure 13. Pressure traces measured in the constant volume explosion experiments for mechanically alloyed Al · Mg powders burning in air. The igniter, a heated wire, is initiated at the time zero.[207]

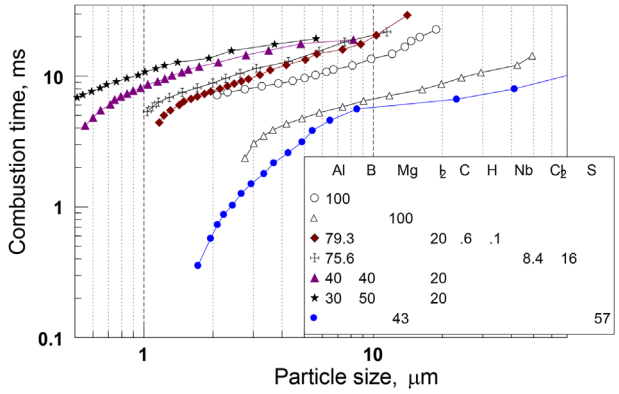

Figure 14. Burn times as a function of particle sizes for some RM powders containing biocidal additives, I_2, Cl_2, or S, burning while being injected in an air-acetylene flame. Results for pure Al and Mg are shown for reference.[208–209]

constrained in a high-pressure diamond anvil cell and others are discussed in a review.[129]

Higher impact energies are achieved in so called Asay shear impact experiment developed originally to test explosives[211] and used to characterize several Ni–Al composite and nanocomposite materials more recently.[212–214] A sample is placed on a support plate; a plunger with a flat impact surface rests on top of the sample. The plunger is hit by a flyer plate accelerated by a gas gun so that it is rapidly pressed into the sample. The impact energies are in the range of hundreds of J. The setup is installed in a windowed chamber so that the ignition can be monitored using a high-speed video camera. In different experiments, impact sensitivities were compared for mixed nanopowders, composites prepared by high-energy ball milling, and for nanolayered composites with the structures generated by magnetron sputtering. It was observed that the porosity and hardness of the samples significantly affected their impact ignition sensitivity, even when their ignition temperatures measured for the heated samples were nearly identical.

In another experimental technique, based on the Taylor test discussed above, a gas gun is used to accelerate a sample of RSM, which impacts onto a stationary anvil.[140,141,215] An RSM sample is attached to a metal carrier rod using custom-manufactured copper capsule fixtures. The powder compact may be pressed into or epoxied to the driver. The flyer plate is made of copper, tungsten, or tungsten heavy alloy, depending on the desired impact stress. The flyer plate is carried by aluminum sabots. The impact velocity is monitored using sequential shorting pins. Polyvinylidene fluoride (PVDF) stress gauge packages are built onto the driver and backer plates to monitor the stress state and wave arrival times at the front and back of the powder. An example of a series of high-speed images for an impact initiation experiment is shown in **Figure 16**.[140] The initiation threshold in terms of impact energy was found for different RM samples. Results for materials prepared as mixtures of regular (not ball milled) powders, suggest that composites of tungsten/aluminum and tantalum/aluminum reacted in both air and vacuum.

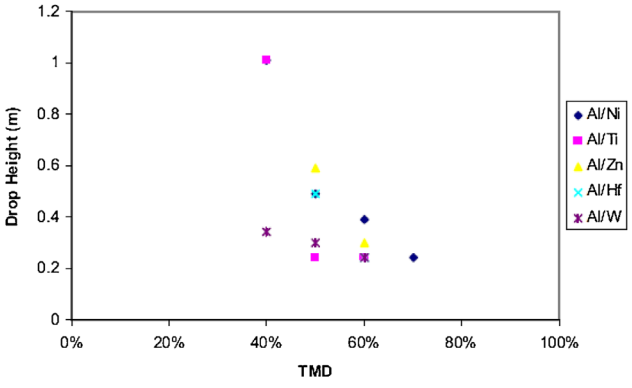

Figure 15. Impact sensitivity of intermetallics measured in air as a function of bulk theoretical maximum density of a pressed sample.[210]

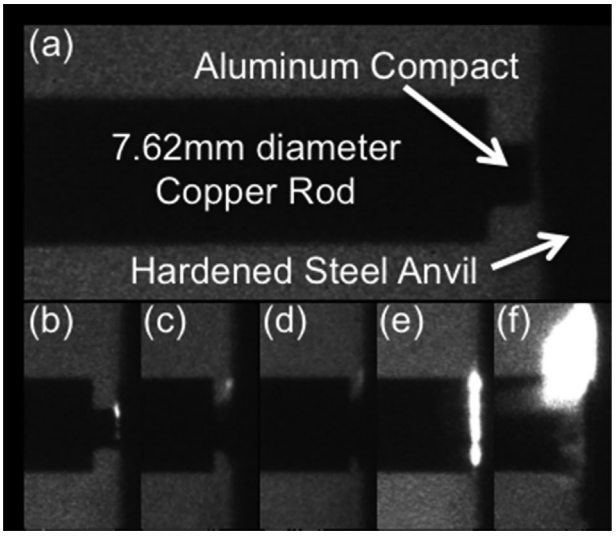

Figure 16. High-speed images of an impact of an RSM projectile onto a hardened steel anvil at 302 m s^{-1}. The RSM is a mechanically milled aluminum compact attached to a copper cylinder. Times corresponding to different frames: a) immediately prior to impact; b–d) 0.05–2.5 μs; e) 6.5 μs; and f) 9.5 μs. Pellet is compacted and deformed in frames b–e). The copper cylinder contacts the anvil in frame (f).[140]

© 2017 WILEY-VCH Verlag GmbH & Co. KGaA, Weinheim

Composites of nickel/aluminum and aluminum compacts only reacted in air[6]; composites of tungsten/aluminum and tantalum/aluminum reacted in both air and vacuum. A higher reactivity was observed for tantalum/aluminum composite. Its reactivity threshold in air was 718 kJ, which was about 195 kJ lower than the next lowest threshold of 913 kJ observed for aluminum. Composites of tungsten/aluminum and nickel/aluminum (at a higher packing density) all react in air at around 1000 kJ. This suggests that aluminum oxidation with surrounding air defines the reaction threshold for all composites except for tantalum/aluminum ones. The intermetallic anaerobic reaction was suggested to be driving tantalum/aluminum compacts. In vacuum, the tantalum/aluminum initiation threshold was 863 kJ, which was 348 kJ lower than that for tungsten/aluminum composite (1211 kJ).

An interesting effect of particle size was observed for nickel/aluminum composites. Samples prepared using powders with different sizes, −325 mesh and +325–200 mesh, exhibited similar trends for the effects of packing density. However, the samples prepared from a coarser powder (+325–200 mesh) were substantially more reactive and initiated at a lower energy than samples prepared using finer, −325 mesh powders.

A customized impact initiation testing methodology was developed a decade ago[216,217] and modified and used in many more recent studies.[4,218–224] In this method, as schematically shown in **Figure 17**,[216] a consolidated RSM compact (which could have spherical, cylindrical, or cubic shape) is used as a projectile. The sample needs to survive launch from a ballistic gun at speeds varied from ca. 500–2500 m s^{-1}. Aluminum foils are used to measure the speed of the projectile. A pressure sensor mounted in the test chamber is not shown. The projectile first hits a "target skin," which is typically a thin sheet of mild steel[216] or an aluminum plate. Some recent experiments are focused on the interaction of RSM with aluminum plates of different thicknesses, production of fragments, and their ignition.[223] Upon passing through the target skin, the RSM projectile is disintegrated. A portion of the material may be left outside the test chamber, while fragments continue moving towards the center of the chamber and impact upon a heavy anvil plate. Ignition occurs upon the impact, resulting in a shock wave and rapid combustion of pulverized material. Although the chamber cannot be sealed because its wall is punctured through by the projectile, the pressure rise in the chamber occurs sufficiently fast to make the pressure measurement meaningful.

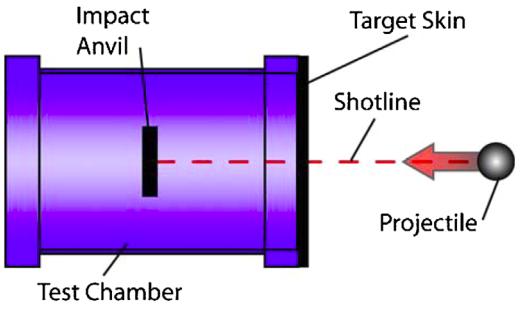

Figure 17. Schematic diagram of an experimental chamber used in the impact initiation experiments by Ames.[216]

The quasistatic pressure (QSP) measured in the chamber upon impact is translated into the energy released. This energy is interpreted considering the theoretical energy release expected from the RSM projectile upon its complete combustion.

Selected results are illustrated in Figure. 18 and 19.[217] Reaction efficiency, measured based on the QSP, increases markedly with increase in the impact speed (**Figure 18**). The effect of density on the reaction efficiency is also very strong, and overarching for a wide range of materials (**Figure 19**). However, all samples represented in Figure 19 were prepared as compacted commercial powders; they do not include more advanced nanocomposite materials.

In addition to the energy release, the minimum impact pressure necessary for ignition of an RSM projectile is identified. For example, the initial critical impact initiated velocity is about 650 m s^{-1} for W/Zr alloy.[224] **Table 1** shows reaction characteristics, including reaction efficiencies for several impact initiated RSM samples. In calculating the kinetic energy, it was assumed

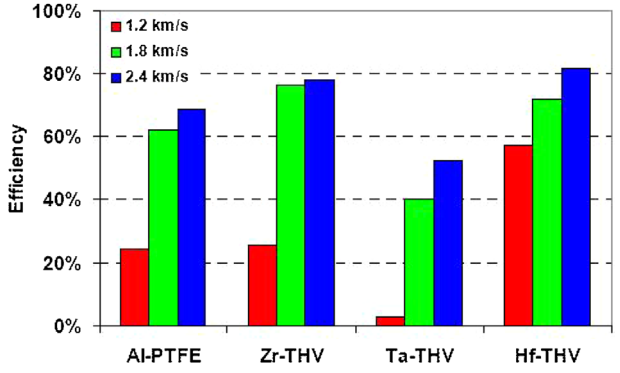

Figure 18. Typical reaction efficiencies for impact initiated RM samples.[217]

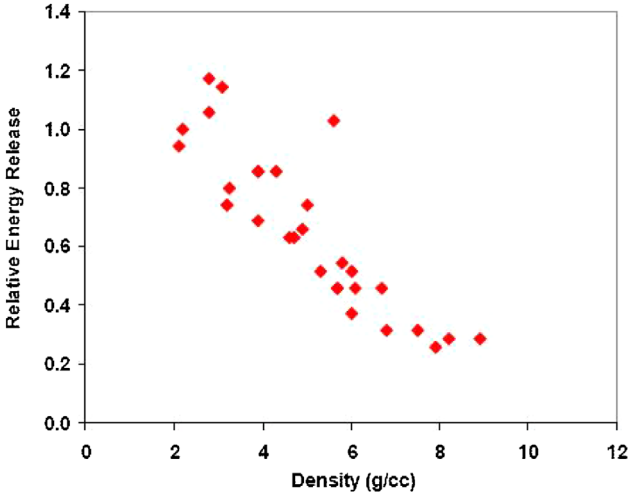

Figure 19. Energy released by different reactive material samples as a function of the material density. The reaction is initiated by a 6,000 ft s^{-1} impact; the energy is normalized by that released by Al-PTFE with TMD of 2.4.[217]

© 2017 WILEY-VCH Verlag GmbH & Co. KGaA, Weinheim

Table 1. Reaction characteristics, including chemical reaction efficiency for different RM compositions tested using an impact of accelerated RM projectile.[224]

Material	Impact velocity (m/s)	Quasi-static pressure (Mpa)	Total energy (kJ)	Kinetic energy (kJ)	Chemical energy (kJ)	Total chemical energy (kJ)	Reaction efficiency (%)	Impact pressure (GPa)
W/Zr	752	0.14	5.46	1.575	3.885	29.145	13.3	12.57
W/Zr	1094	0.21	8.19	3.384	4.806	29.895	16.1	19.29
W/Zr	1335	0.45	17.55	5.004	12.546	29.359	42.7	24.40
Al/PTFE	847	0.10	3.90	2.124	1.776	25.314	7.0	5.49
Al/PTFE	934	0.19	7.41	2.520	4.890	24.041	20.0	6.19
Al/PTFE	1004	0.30	11.70	3.141	8.559	26.021	32.9	6.76
Al/PTFE	1203	0.68	26.52	4.320	22.200	25.879	85.8	8.49
Al/PTFE	1481	0.23	8.97	6.867	2.103	26.304	8.0	11.09
Al	1049	0.07	2.73	3.456	...	...	...	...
Al	1169	0.08	3.12	4.311	...	...	...	...

that the samples entered the chamber at 90% of their initial kinetic energy after passing through the target skin.

In recent experiments following the same general approach, the RSM was packed into a reactive bullet, as a reactive fragment inside a steel shell.[225] The impact initiation behavior of Al/PTFE RSMs with added tungsten was investigated. It was found that a greater reaction efficiency was achieved at higher impact velocity. Samples with greater porosities and with greater concentration of tungsten were more reactive. Tungsten was not observed to participate in the reaction, however.

5.3.4. Explosive Initiation of RSMs

Initiation of RSM samples using an explosive is aimed to imitate a scenario when the RSM serves as a case or liner for a munition carrying an explosive charge. Efforts[226,227] was aimed to observe detonations in consolidated RSM samples. Qualitatively similar experimental configurations were used, as shown schematically in **Figure 20**. An RSM sample was constrained in a thick-walled container. To minimize the effect of reflected sound waves on the measurements dealing with Zn–S composition, the container was made of a porous composite with a low sound speed.[227] In both studies,[226,227] the results were inferred from the velocity measurements for the propagating combustion wave. It was concluded that a detonation wave was possible for an RSM system with the minimized gas release, for which both reactants and products were condensed phases.

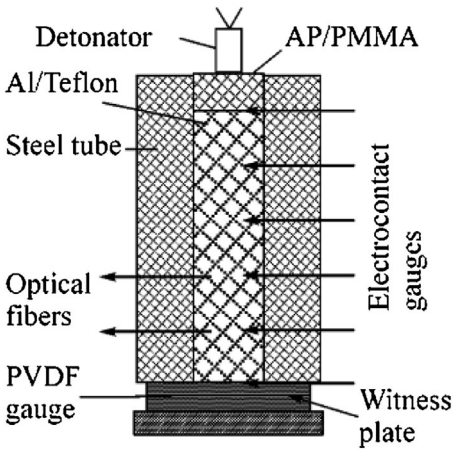

Figure 20. An experiment studying an explosive-driven detonation in an aluminum-PTFE composite.[226]

In other studies,[228,229] a qualitatively similar experimental setup was built and used to consider a detonation-induced reaction in the Zn–S samples prepared at different nominal densities, as illustrated in **Figure 21**. Dimensions of the RSM samples were increased to enable recovery and analysis of the materials after the experiments. Despite the larger sample size, no self-accelerated reaction rates were observed. It was, therefore, concluded that no evidence for gasless detonation currently exists.

A set of experiments described in refs.[230,231] followed up on extensive earlier work aimed to identify the mechanism of initiation and propagation of a shock initiated reaction in a condensed phase RSM. The general focus of this work was to establish the size of the area directly initiated by the shock, often referred to as a hot spot, and to determine the mechanism of the reaction propagation through the rest of material. Two experimental configurations shown in **Figure 22** were used.[230] In both cases, an RSM sample was constrained in a cylindrical steel capsule. An explosive placed on top of the capsule was detonated. In one of the configurations, Figure 22a, both thermocouple and light sensor were used to monitor reaction. In this case, a polycarbonate window was used as part of the sample enclosure; the explosive charge in this case was limited to 130 g of nitromethane (NM) sensitized with 5 wt% of diethylenetriamine. It was expected that the optical signal will show when local high temperatures occur, for example, when hot spots are formed. Conversely, the thermocouples were expected to describe the rise in the bulk sample temperature when the reactions propagate. In the configuration shown in Figure 22b, only thermocouples were used and the window was replaced by a steel part. In the latter case, the explosive was 450 g of commercial pentolite. Yet another experimental configuration

© 2017 WILEY-VCH Verlag GmbH & Co. KGaA, Weinheim

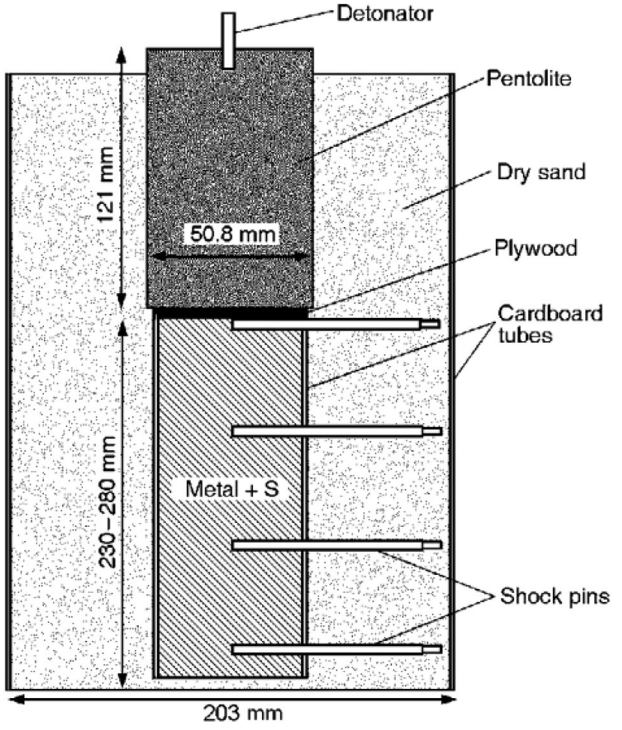

Figure 21. Experimental setup used to study an explosive driven reactions in different RMs.[229]

was used, when only optical signal was collected. For these experiments, the light passed through a hole drilled in a steel component, while the entire capsule was placed in a water pool. After experiments, samples were recovered to observe the extent of reaction. Some of the recovered samples were completely reacted; for others, no evidence of bulk initiation was observed. No partially reacted materials were found.

Based on results of the experiments, it was concluded that the initiation of hot spots occurs in the time scale of μs, comparable to the time of shock compression. Conversely, reaction propagation occurs at a much longer time scale, from ms to hundreds of ms. The burn rate in such materials was found to be largely pressure-independent.

In a complementary study,[231] shock initiation was studied for a broad range of samples with the focus on correlation between thermal and shock initiation processes. The process of ball-milling or mechanical activation was found to increase both thermal and shock sensitivity. It was further found that the increased thermal sensitivity was not caused by shock compression alone. For samples shocked at pressures just lower than necessary for ignition, the ignition threshold was found to be indistinguishable from the equivalent un-shocked samples.

Shock initiation of laminate Ni–Al composite samples was studied using so called "Thick-Walled Cylinder Method" presented schematically in **Figure 23**.[232,233] A cylindrical RSM sample is placed inside a copper tube. The assembly is placed inside PVC container filled with an explosive. The information about reaction initiation is obtained by recovery and examination of the samples following the experiments. The focus is on the mechanical processes leading to chemical reactions. It was established that instabilities during the collapse of the Ni–Al-corrugated laminate composites triggered three main mechanisms of plastic strain accommodation. The inside facing wedge-shaped regions at the inner surface of the laminate were extruded. There was a small number of non-uniformly distributed local/global trans-layer shear bands. The initial locally concentric layers experienced cooperative buckling. These mechanisms were specific to the configuration studied and different from shear localization processes involving plastic deformation and discussed in earlier work with fully dense or granular materials.

A different set of experiments with shock-initiated RSMs addresses applications, in which an RSM is dispersed and initiated by interaction with a shock wave produced by a high explosive (HE).[27,37,234] In one of the experiments, a pressed pellet of mechanically alloyed B–Ti powder was placed directly

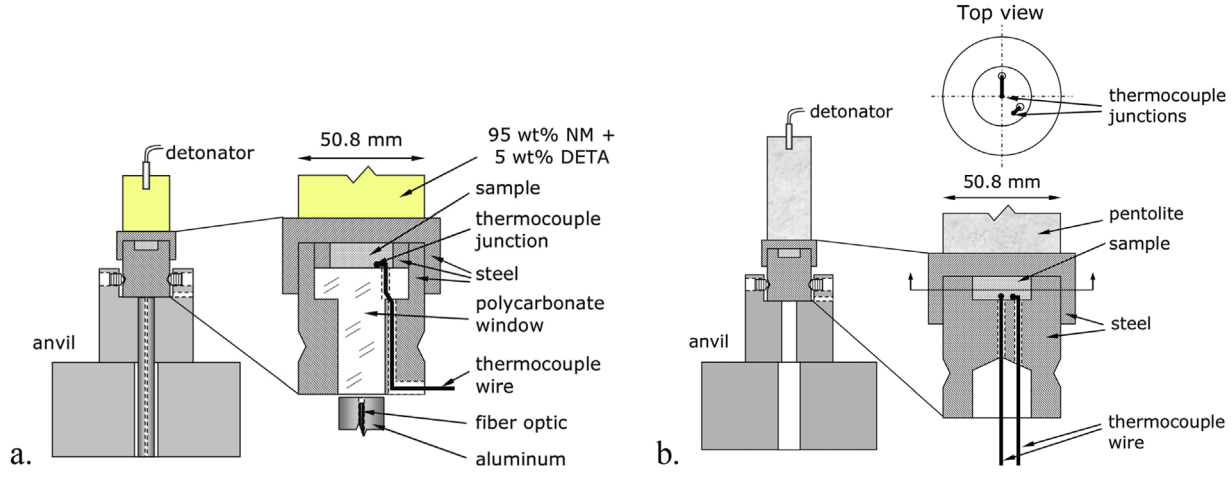

Figure 22. Experimental configurations used in ref.[230] for explosive-initiated experiments with RMs. A) Experiments with photo-multiplier tubes and thermocouples; b) experiments with thermocouples.

© 2017 WILEY-VCH Verlag GmbH & Co. KGaA, Weinheim

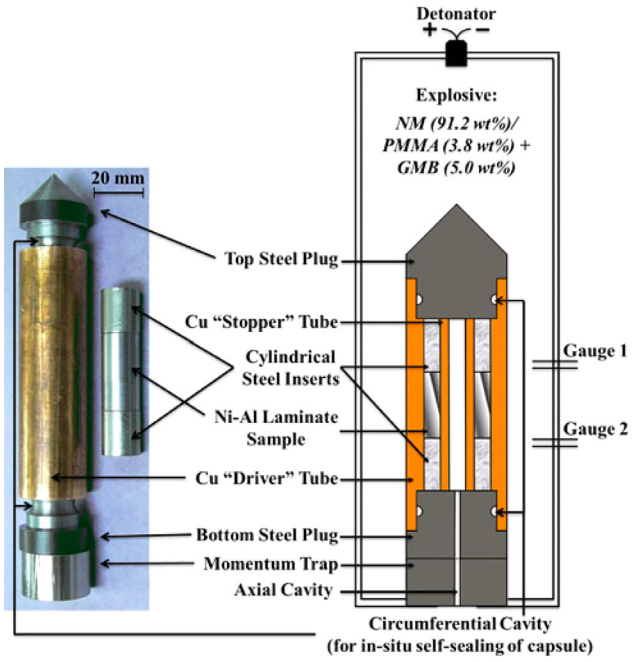

Figure 23. Experimental configuration for the thick walled cylinder method.[232–233] See https://doi.org/10.1080/14786435.2014.948524 for details.

on top of an HE pellet. The experiments were performed in a chamber with optical ports for high speed video and spectroscopy. The chamber was also equipped with both transient and QSP transducers. It was observed that the mechanically alloyed materials produced greater pressure and greater energy release than other samples with the same bulk compositions (blended powders or titanium boride). The method used to prepare mechanically alloyed material was found to be critical to ensure the best performance. In other experiments, a conceptually similar configuration generating a more spatially uniform explosion was used for testing mechanically alloyed W–Zr samples.[37] Disk-shaped 12.7-mm diameter pellets of RSM pressed to 60–70%TMD were arranged to form a dodecahedron. A 18-g nitromethane charge used to initiate the RSM was located at the geometrical center. Experiments were performed inside a $1.2\,m \times 1.2\,m \times 1.2\,m$ steel blast chamber. Both transient and QSP measurements were made. Results were processed to estimate the completeness of tungsten combustion based on the net QSP-implied energy release. The net QSP was obtained by reducing the measured QSP by that obtained in tests with the nitromethane charge and inert tungsten oxide pellets instead of RSM. A bare Zr case was used as a reference for RSM assessment. In the reference experiment, QSP suggested that approximately 86% of the theoretical energy of Zr combustion was released. The calculated and measured energy release is illustrated in Figure 24.[37] If the only reaction is that of Zr, the calculated energy release becomes smaller when W is added. The decay as a function of W concentration is predicted even if 75% of the added W combusts. The present results suggest no decay, or, in fact a slight increase in the QSP with tungsten combustion. Thus, a nearly 100% reaction efficiency is implied. This reaction occurs in the time scale of 20–100 ms (**Figure 24**).

In recent studies,[37,234,235] an experimental configuration involving a cylindrical liner of an RM powder initiated by a centrally placed explosive charge, as shown in **Figure 25** was explored. Fragmentation of a pressed aluminum case was studied in ref.,[235] while both aluminum and differently prepared Al–Mg composites were used in the reactive liners in ref.[234] It was found that the explosion leads to compaction of the aluminum powder to near solid density, and its subsequent fracture into fragments that are several centimeters long and less than a centimeter thick.[235] Reactive liners were prepared with pure aluminum, cast alloyed and mechanically alloyed Al · Mg powders, and with blended Al and Mg powders. For reference, liners were also prepared filled with inert Al_2O_3 powder. All liners filled with reactive powders produced higher QSP than the inert reference; they also exhibited a stronger initial pressure peak occurring in the sub-millisecond time scale, important for improvement of the air blast characteristics. In particular, both time of arrival of the pressure peak and its amplitude were improved in experiments with reactive liners. The mechanically

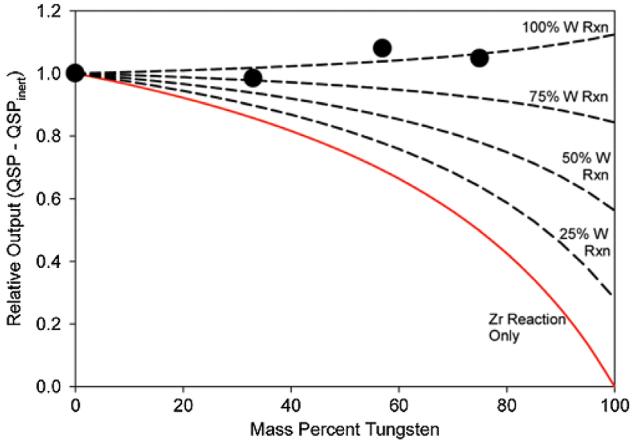

Figure 24. Net QSP is the total QSP minus that of the test with inert (WO_3) pellets. Measured net QSP produced by W–Zr alloys normalized to the pure Zr case.[37] Dashed lines show expected net QSP for different degrees of tungsten reaction.

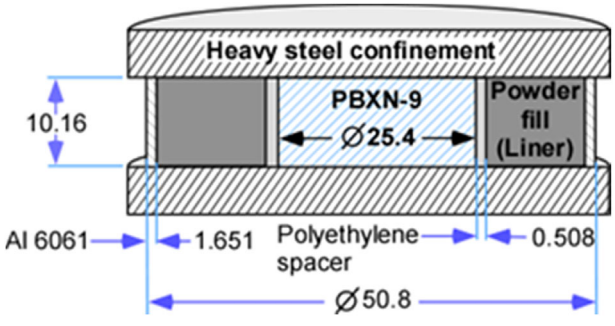

Figure 25. Charge configuration for reactive liners with a PBXN-9 booster used in experiments.[234] Dimensions are in mm.

© 2017 WILEY-VCH Verlag GmbH & Co. KGaA, Weinheim

alloyed powder showd the most significant improvement in the early blast characteristics, although it did not offer substantial benefits in terms of QSP, as compared to the pure Al. These results are interesting as direct indicators that a very rapid reaction is possible for RSMs, which could usefully contribute to the early blast development. The mechanisms of such prompt metal combustion are not understood presently and further work is desired to determine such mechanisms and exploit them for design of optimized RSMs.

6. Summary and Future Work

Metal-based compositions capable of various self-sustaining exothermic reactions have been prepared and tested for potential use in applications requiring both structural strength and ability to generate chemical energy upon initiation by heat, impact, or shock. Such materials, referred to as reactive structural materials, emerged as an important group of composites, prepared by multiple methods and required customized characterization approaches. The composites can react forming oxides, fluorides, carbides, borides, sulfides, silicides, and aluminides. They are prepared by mixing starting powders or nanopowders, employing binders, mechanically refining bulk metals or powders of starting materials, and by layered deposition of starting elements or molecules. Consolidating composites prepared as powders is an important step in designing RSMs, where both high density and reactivity are desired. Contemporary approaches, such as involving additive manufacturing and enabling design of customized material architectures are of particular interest.

Chemically, the most reactive systems are those relying on the reactions of oxidation and fluorination; however, typically materials relying on such reactions have relatively low densities or require an external oxidizer. Including a high-density additive, such as tungsten, is relatively common; however, such additive is chemically inert in most cases. Advanced refining methods, such as high energy mechanical milling or preparation of layered structures by magnetron sputtering generates useful, high density morphologies, which hold promise of combining the high density and reactivity for the future RSMs.

Both mechanical and energetic properties of RSMs must be characterized. Traditional characterization methods, such as static mechanical testing and thermal analysis are necessary, but must be supplemented by dynamic experiments. In mechanical tests, such as using SHPB, initiation of RSMs is probed in addition to recovery of their dynamic mechanical properties. In addition, customized test methods, addressing, for example, fragmentation of the RSMs upon impact and reactivity of the produced fragments are developed and used for a broad range of RSM compositions. These experiments are usefully supplemented with the studies focused on ignition and combustion of individual particles and meso-particles, used to prepare consolidated RSMs and expected to re-emerge upon the RSM fragmentation. Results of the latter studies may be used to predict the behavior of RSM fragments in various practical scenarios. Little is presently done to characterize long-term stability and aging of RSM composites, and work is expected in that direction, involving advanced thermal analysis and microcalorimetry.

Dynamic initiation experiments for RSMs described in the literature currently can be seen as two distinct groups: one, dealing with microscopic samples and involving very fine spatial and temporal scales, and the other, dealing with relatively large consolidated samples exposed to conditions expected in a practical application. Presently, there is essentially no link between the outputs of these different types of experiments. It is hoped that a better connection can be developed in the future. In particular, using the same types of RSMs in different types of tests and comparing results systematically should be useful.

The theoretical ideas describing fragmentation and reactions in RSMs are much less developed presently and were not reviewed here. Such descriptions are necessary, however, and future experiments should be designed to enable and support development of the relevant models. The models should describe both mechanical and energetic properties of the new materials and must be compatible with the state of the art hydrodynamic codes describing munition systems in which the use of RSMs is anticipated.

The work aimed at developing new RSM compositions is expected to continue and focus on ternary and more complex materials systems. It is further expected that advanced materials processing and consolidation techniques, such as mechanical milling, layered deposition, controlled isostatic pressing, cold spray, and others will be combined to prepare final advanced RSM structures. Materials with modulated densities and tunable heat release kinetics are of particular interest.

Acknowledgement

This work was supported in parts by the US Defense Threat Reduction Agency and Air Force Office of Scientific Research.

Conflict of Interest

The authors declare no conflict of interest.

Keywords

composite materials, ignition, intermetallics, metal combustion, thermal analysis, thermites

Received: July 26, 2017
Revised: August 26, 2017
Published online:

[1] T. Ackerman, D. R. Crofts, K. Gulia, M. M. M. Attallah, Patent GB2526262A, **2015**.
[2] J. Chen, B. H. Yuan, Z. F. Liang, C. Xiao, Y. J. Chen, *Huozhayao Xuebao/Chin. J. Explos. Propellants* **2015**, *38*, 49.
[3] J. P. Hooper, *J. Appl. Phys.* 043508, **2012**, *112*, DOI: 10.1063/1.4746788.
[4] R. J. Lee, W. Mock, Jr., J. R. Carney, W. H. Holt, G. I. Pangilinan, R. M. Gamache, J. M. Boteler, D. G. Bohl, J. Drotar, G. W. Lawrence, *AIP Conf. Proc.* **2006**, *845*, 169.
[5] D. B. Nielson, R. M. Truitt, B. N. Ashcroft,. EP1780494A2, United States Patent 8122833, published 02/28/2012.

 © 2017 WILEY-VCH Verlag GmbH & Co. KGaA, Weinheim

[6] M. D. Tucker, *Characterization of impact initiation of aluminum-based intermetallic-forming reactive materials*. MS Thesis, Georgia Institute of Technology, Atlanta, GA, **2011**.
[7] F. Zhang, M. Gauthier, C. Cojocaru, *Propellants Explos. Pyrotech*. **2017**, *42*, 1.
[8] W. Q. Wan, D. Q. Yu, F. Peng, W. M. Wang, T. H. Yang, *Baozha Yu Chongji/Explos. Shock Waves* **2014**, *34*, 235.
[9] J. Liou, G. H. Huang, Y. -Y. You, M.-T. Hsu, *Huoyao Jishu* **2012**, *28*, 35.
[10] Z. Wang, Y. Li, H. Wang, W. Wang, Z. Hou, *J. Chem. Pharma. Res*. **2014**, *6*, 287.
[11] Q. B. Yu, Z. W. Liu, X. K. Jin, H. F. Wang, *Beijing Ligong Daxue Xuebao/Trans. Beijing Inst. Technol*. **2012**, *32*, 661.
[12] V. L. Bucharskiy, P. V. Frolov, *Assessment of use of active-reactive munition charge by method of integral approximation. Bulletin of Dnepropetrovsk University; Series: Space rocket technology (In Ukrainian)* **2012**, *20*, 38.
[13] M. Mayseless, *J. Appl. Mech. Trans. ASME* 051006, **2011**, 78.
[14] H. N. G. Wadley, K. P. Dharmasena, M. Y. He, R. M. McMeeking, A. G. Evans, T. Bui-Thanh, R. Radovitzky, *Int. J. Impact Eng*. **2010**, *37*, 317.
[15] F. Zhang, W. Wilson, *Shock Compress. Condens. Matter* **2009**, pp.149-152.
[16] F. Zhang, R. Ripley, W. H. Wilson, *Air Blast Characteristics of Laminated al and NI-AL Casings*, AIP Conf. Proceedings, Volume *1426*, Issue 1. Paper number 10.1063/1.3686272, **2012**; p. 275.
[17] S. P. Li, G. Y. Huang, S. S. Feng, C. Wang, H. Zou, *Binggong Xuebao/Acta Armamentarii* **2011**, *32*, 57.
[18] C. Mitsakou, K. Eleftheriadis, C. Housiadas, M. Lazaridis, *Health Phys*. **2003**, *84*, 538.
[19] R. J. Lee, W. Mock Jr, J. R. Carney, W. H. Holt, Pangilinan, R. M. Gamache, J. M. Boteler, D. G. Bohl, J. Drotar, G. W. Lawrence, *AIP Conf. Proc*. **2006**, *845,* p. 169.
[20] B. Zygmunt, *Hanneng Cailiao/Chin. J. Energetic Mater*. **2007**, *15*, 592.
[21] A. Bacciochini, M. I. Radulescu, M. Yandouzi, G. Maines, J. J. Lee, B. Jodoin, *Surf. Coat. Technol*. **2013**, *226*, 60.
[22] A. Ermoline, Y. Aly, M. A. Trunov, M. Schoenitz, E. L. Dreizin, *Int. J. Energetic Mater. Chem. Propul*. **2010**, *9*, 267.
[23] P. Dupiano, D. Stamatis, E. L. Dreizin, *Int. J. Hydrogen Energy* **2011**, *36*, 4781.
[24] S. W. Du, B. Aydelotte, D. Fondse, C. T. Wei, F. Jiang, E. Herbold, K. Vecchio, M. A. Meyers, N. N. Thadhani, *AIP Conf. Proc*. **2009**, *1195*, p. 498. https://doi.org/10.1063/1.3295183
[25] B. Aydelotte, N. N. Thadhani, *Mater. Res. Soc. Symp. Proc.*, **2013**; p. 13. Materials Research Society (MRS), Boston MA.
[26] A. Bacciochini, S. Bourdon-Lafleur, C. Poupart, M. Radulescu, B. Jodoin, *J. Therm. Spray Technol*. **2014**, *23*, 1142.
[27] M. D. Clemenson, S. Johnson, H. Krier, N. Glumac, *Propellants Explos. Pyrotech*. **2014**, *39*, 454.
[28] N. A. Kochetov, S. G. Vadchenko, *Combust. Explos. Shock Waves* **2015**, *51*, 467.
[29] V. Rosenband, B. Natan, A. Gany, *J. Propul. Power* **1995**, *11*, 1125.
[30] M. A. Trunov, V. K. Hoffmann, M. Schoenitz, E. L. Dreizin, *J. Propul. Power* **2008**, *24*, 184.
[31] I. Song, L. Wang, M. Wixom, L. T. Thompson, *J. Mater. Sci*. **2000**, *35*, 2611.
[32] H. Ren, X. Liu, J. Ning, *Mater. Sci. Eng. A* 115205 **2016**, *660*, 205.
[33] H. Ren, X. Liu, J. Ning, *AIP Adv*. **2016**, *6*, DOI: 10.1063/1.4967340.
[34] L. Z. Xu, Z. H. Du, *Key Eng. Mater*. **2017**; Vol. 723 KEM, p. 202.
[35] H. Zhang, J. Yin, Z. Wang, *Appl. Mech. Mater*. **2012**; Vol. 217–219, p. 358.
[36] J. S. Zhu, Z. Fan, B. Gao, *Adv. Mater. Res*. **2014**; Vol. 936, p. 1927.
[37] A. Coverdill, C. Delaney, A. Jennrich, H. Krier, N. G. Glumac, *J. Energetic Mater*. **2014**, *32*, 135.
[38] L. J. Kecskes, K. A. Darling, *Proc. of the 8th Int. Conf. Tungsten Refract. Hard Mater*. **2011**, Elsevier B.V., San Fransisco, CA, p 936.
[39] M. W. Chase, *J. Phys. Chem. Ref. Data, Monograph 9* **1998**, 1.
[40] S. H. Fischer, M. C. Grubelich, *Proc. Int. Pyrotech. Seminar, 24th* **1998**, 231.
[41] K. T. Jacob, A. Kumar, G. Rajitha, Y. Waseda, *High Temp. Mater. Processes* **2011**, *30*, 459.
[42] S. V. Meschel, O. J. Kleppa, *J. Alloys Compd*. **1997**, *257*, 227.
[43] E. S. Domalski, G. T. Armstrong, *Heats of Formation of Metallic Borides by Fluorine Bomb Calorimetry*; Report APL-TDR-64-39, Air Force Aero Propulsion Laboratory, Research and Technology Division, Air Force Systems Command Wright-Patterson Air Force Base, Ohio, **1964**; p 75.
[44] E. Rudzitis, R. Terry, H. M. Feder, W. N. Hubbard, *J. Phys. Chem*. **1964**, *68*, 617.
[45] B. E. Douda, *Survey of Military Pyrotechnics*; Naval Weapons Support Center Ordnance Engineering Department Crane, IN, **1991**, p 41. Report NWSC/CR/RDTR-595.
[46] M. L. Chan, G. W. Meyers, *Adv. Thermobaric Explos. Compos*. US Patent US6955732, **2005**.
[47] W. S. Rossett, *An Overview of Novel Penetrator Technology*; Report ARL-TR-2395; Army Research Laboratory: Aberdeen Proving Ground, MD, **2001**.
[48] J. Askill, *Tracer Diffusion Data for Metals, Alloys, and Simple Oxides*. New York, IFI/Plenum, 1970. **1970**.
[49] H. Nakajima, W. Sprengel, K. Nonaka, *Intermetallics* Volume 4, Supplement 1, **1996**, S17.
[50] S. T. Frank, S. V. Divinski, U. Sodervall, C. H. R. Herzig, *Acta Mater*. **2001**, *49,* 1399.
[51] M. Keddam, S. Taktak, S. Tasgetiren, *Surf. Eng*. **2016**, *32*, 802.
[52] Q. Fu, T. Wagner, *Surf. Sci. Rep*. **2007**, *62*, 431.
[53] A. Atkinson, *Rev. Mod. Phys*. **1985**, *57*, 437.
[54] M. W. Beckstead, *Combust. Explos. Shock Waves* **2005**, *41*, 533.
[55] Y. Aly, V. K. Hoffman, M. Schoenitz, E. L. Dreizin, *Mater. Res. Soc. Symp. Proc*. **2013**; p 43. MRS, Boston, MA.
[56] A. Maček, J. M. Semple, *Symp. (Int.) Combust*. **1971**, *13*, 859.
[57] K. -L. Chintersingh, Q. Nguyen, M. Schoenitz, E. L. Dreizin, *Combust. Flame* **2016**, *172*, 194.
[58] G. Young, K. Sullivan, M. R. Zachariah, K. Yu, *Combust. Flame* **2009**, *156*, 322.
[59] I. E. Molodetsky, E. P. Vicenzi, E. L. Dreizin, C. K. Law, *Combust. Flame* **1998**, *112*, 522.
[60] E. Shafirovich, S. K. Teoh, A. Varma, *Combust. Flame* **2008**, *152*, 262.
[61] S. Wang, S. Mohan, E. L. Dreizin, *Combust. Flame* **2016**, *168*, 10.
[62] X. Huang, Z. -X. Xia, L. -Y. Huang, J. X. Hu, *Hanneng Cailiao* **2013**, *21*, 379.
[63] H. M. Cassel, I. Liebman, *Combust. Flame* **1962**, *6*, 153.
[64] E. L. Dreizin, C. H. Berman, E. P. Vicenzi, *Combust. Flame* **2000**, *122*, 30.
[65] S. Wang, A. L. Corcoran, E. L. Dreizin, *Combust. Flame* **2015**, *162*, 1316.
[66] A. Saigal, V. S. Joshi, *Am. Soc. Mech. Eng. Press. Vessels Pip. Div. (Publication) PVP* **2000**, *432*, 107.
[67] V. S. Joshi, *Process for Making Polytetrafluoroethylene-Aluminum Composite and Sintered Product Made*. US6547993B1, **2003,** 25–29, 6.
[68] a) J. Wu, M. Li, S. Zhang, Y. Mei, Z. Gao, *Adv. Mater. Res. (Durnten-Zurich, Switz.)* **2013.**
[69] S. Q. Yang, S. L. Xu, T. Zhang, *Guofang Keji Daxue Xuebao* **2008**, *30*, 39.
[70] C. Ge, W. Maimaitituersun, Y. Dong, C. Tian, *Materials* **2017**, *10*.
[71] Z. Lu, D. Jiang, P. Tang, *BALLISTICS 2014: 28th Int. Symposium on Ballistics* (Eds: G. Richard, R. Daniel Boeka), Publisher: DEStech Publications, Inc., Lancaster, PA **2014**.

 © 2017 WILEY-VCH Verlag GmbH & Co. KGaA, Weinheim

[72] J. Cai, V. F. Nesterenko, K. S. Vecchio, E. B. Herbold, D. J. Benson, F. Jiang, J. W. Addiss, S. M. Walley, W. G. Proud, *Appl. Phys. Lett*. **2007,** *92*, 1, paper 10.1063/1.2832672.
[73] G. Young, C. A. Stoltz, D. H. Mayo, C. W. Roberts, C. L. Milby, *Combust. Sci. Technol*. **2013**, *185*, 1261.
[74] D. B. Nielson, R. M. Truitt, R. D. Poore, B. N. Ashcroft, *Reactive Material Compositions for Shot Shells Ammunition Consisting of Metal Fuels, Inorganic Oxidants, Epoxy resins, and Fluoropolymer Binders*. US20070272112A1, **2007**.
[75] B. E. Homan, K. L. McNesby, J. Ritter, J. Colburn, A. Brant, *Characterization of the Combustion Behavior of Aluminum-Nickel Based Reactive Materials*; Report ARL-TR-4917, Weapons and Material Research Directorate, ARL: Aberdeen Proving Ground, MD 21005, **2009**.
[76] J. D. Gibbins, A. K. Stover, N. M. Krywopusk, K. Woll, T. P. Weihs, *Combust. Flame* **2015**, *162*, 4408.
[77] T. F. Zahrah, R. Rowland, L. Kecskes, *High-Density Hf-Base and Fe-Based Metallic-Glass-Alloy Powders and Their Composite Derivatives*. US20060062684A1, **2006**.
[78] S. W. Dean, J. K. Potter, R. A. Yetter, T. J. Eden, V. Champagne, M. Trexler, *Intermetallics* **2013**, *43*, 121.
[79] V. F. Nesterenko, P. H. Chiu, C. Braithwaite, A. Collins, D. Williamson, K. L. Olney, D. B. Benson, F. McKenzie, *AIP Conf. Proc*. *1426*, **2012**; p 533.
[80] P. H. Chiu, V. F. Nesterenko, *J. Compos. Mater*. **2016**, *50*, 4015.
[81] P. H. Chiu, K. S. Vecchio, V. F. Nesterenko, *Int. J. Impact Eng*. **2017**, *100*, 1.
[82] E. S. Collins, B. R. Skelton, M. L. Pantoya, F. Irin, M. J. Green, M. A. Daniels, *Combust. Flame* **2015**, *162*, 1417.
[83] M. L. Pantoya, S. W. Dean, *Thermochimica Acta* **2009**, *493*, 109.
[84] C. D. Yarrington, S. F. Son, T. J. Foley, S. J. Obrey, A. N. Pacheco, *Propellants Explos. Pyrotech*. **2011**, *36*, 551.
[85] R. A. Yetter, G. A. Risha, S. F. Son, *Proc. Combust. Inst*. **2009**, *32 II*, 1819.
[86] D. Erdeniz, G. Gulsoy, D. Colanto, T. Ando, *Ignition Characteristics of Aluminum-Nickel Heterostructures Produced by Ultrasonic Powder Consolidation*, in TMS 2010, *Ann. Meeting Exhibition, Miner. Met. Mater. Soc.*: **2010**; p 729.
[87] S. Gheybi Hashemabad, T. Ando, *Combust. Flame* **2015**, *162*, 1144.
[88] S. K. Pillai, A. Hadjiafxenti, C. C. Doumanidis, T. Ando, C. Rebholz, *Int. J. Appl. Ceram. Technol*. **2012**, *9*, 206.
[89] B. J. Clapsaddle, L. Zhao, A. E. Gash, J. H. Satcher Jr, K. J. Shea, M. L. Pantoya, R. L. Simpson, In *Synthesis and Characterization of Mixed Metal Oxide Nanocomposite Energetic Materials*, MRS Proceedngs 800, R. Armstrong, N. Thadhani, W. Wilson, J. Gilman, R. Simpson, Eds. Boston, MA., 2003; p. 91.
[90] A. E. Gash, J. H. Satcher Jr, R. L. Simpson, B. J. Clapsaddle, *Nanostructured Energetic Materials with Sol-Gel Methods*, in MRS Proceedings 800, R. Armstrong, N. Thadhani, W. Wilson, J. Gilman, R. Simpson, Eds. MRS, Boston, MA, 2003; p. 55.
[91] K. B. Plantier, M. L. Pantoya, A. E. Gash, *Combust. Flame* **2005**, *140*, 299.
[92] D. Prentice, M. L. Pantoya, A. E. Gash, *Energy Fuels* **2006**, *20*, 2370.
[93] J. L. Cheng, H. H. Hng, H. Y. Ng, P. C. Soon, Y. W. Lee, *J. Phys. Chem. Solids* **2010**, *71*, 90.
[94] R. Thiruvengadathan, S. W. Chung, S. Basuray, B. Balasubramanian, C. S. Staley, K. Gangopadhyay, S. Gangopadhyay, *Langmuir* **2014**, *30*, 6556.
[95] J. L. Cheng, H. H. Hng, Y. W. Lee, S. W. Du, N. N. Thadhani, *Combust. Flame* **2010**, *157*, 2241.
[96] J. L. Cheng, H. H. Hng, H. Y. Ng, P. C. Soon, Y. W. Lee, *J. Phys. Chem. Solids* **2010**, *71*, 90.
[97] X. Li, P. Guerieri, W. Zhou, C. Huang, M. R. Zachariah, *ACS Appl. Mater. Interfaces* **2015**, *7*, 9103.
[98] X. Zhou, M. Torabi, J. Lu, R. Shen, K. Zhang, *ACS Appl. Mater. Interfaces* **2014**, *6*, 3058.
[99] K. T. Sullivan, C. Zhu, E. B. Duoss, A. E. Gash, D. B. Kolesky, J. D. Kuntz, J. A. Lewis, C. M. Spadaccini, *Adv. Mater. (Deerfield Beach, Fla.)* **2016**, *28*, 1934.
[100] K. T. Sullivan, C. Zhu, D. J. Tanaka, J. D. Kuntz, E. B. Duoss, A. E. Gash, *J. Phys. Chem. B* **2013**, *117*, 1686.
[101] A. M. Marquez, C. H. Braithwaite, T. P. Weihs, N. M. Krywopusk, D. J. Gibbins, K. S. Vecchio, M. A. Meyers, *J. Appl. Phys*. 145903, **2016**, *119*, DOI: 10.1063/1.4945813.
[102] D. P. Adams, *Thin Solid Films* **2015**, *576*, 98 (Copyright (C) 2014 American Chemical Society (ACS). All Rights Reserved.), Ahead of Print.
[103] M. E. Reiss, C. M. Esber, D. van Heerden, A. J. Gavens, M. E. Williams, T. P. Weihs, *Mater. Sci. Eng. A* **1999**, *261*, 217.
[104] A. J. Gavens, D. van Heerden, A. B. Mann, M. E. Reiss, T. P. Weihs, *J. Appl. Phys*. **2000**, *87*, 1255.
[105] S. C. Barron, S. T. Kelly, J. Kirchhoff, R. Knepper, K. Fisher, K. J. T. Livi, E. M. Dufresne, K. Fezzaa, T. W. Barbee, T. C. Hufnagel, T. P. Weihs, S. C. Barron, S. T. Kelly, J. Kirchhoff, R. Knepper, K. Fisher, K. J. T. Livi, E. M. Dufresne, K. Fezzaa, T. W. Barbee, T. C. Hufnagel, T. P. Weihs, *J. Appl. Phys*. 223517, **2013**, *114* DOI: 10.1063/1.4840915.
[106] G. M. Fritz, G. M. Fritz, S. J. Spey Jr., M. D. Grapes, T. P. Weihs, J. *Appl. Phys. (Melville, NY, U. S.)* 014901, **2013**, *113* (Copyright (C) 2014 American Chemical Society (ACS). All Rights Reserved.), 014901/1-014901/11.
[107] K. J. Blobaum, M. E. Reiss, J. M. Plitzko Lawrence, T. P. Weihs, *J. Appl. Phys*. **2003**, *94*, 2915.
[108] K. J. Blobaum, A. J. Wagner, J. M. Plitzko, D. van Heerden, D. H. Fairbrother, T. P. Weihs, *J. Appl. Phys*. **2003**, *94*, 292.
[109] J. Kwon, J. M. Ducéré, P. Alphonse, M. Bahrami, M. Petrantoni, J. F. Veyan, C. Tenailleau, A. Estève, C. Rossi, Y. J. Chabal, *ACS Appl. Mater. Interfaces* **2013**, *5*, 605.
[110] A. Nicollet, G. Lahiner, A. Belisario, S. Souleille, M. Djafari-Rouhani, A. Estève, C. Rossi, *J. Appl. Phys*. 034503, **2017**, *121* DOI 10.1063/1.4974288.
[111] M. Petrantoni, C. Rossi, L. Salvagnac, V. Conédéra, A. Estève, C. Tenailleau, P. Alphonse, Y. J. Chabal, *J. Appl. Phys*. 084323, **2010**, *108*.
[112] C. Lanthony, M. Guiltat, J. M. Ducéré, A. Verdier, A. Hémeryck, M. Djafari-Rouhani, C. Rossi, Y. J. Chabal, A. Estève, *ACS Appl. Mater. Interfaces* **2014**, *6*, 15086.
[113] L. Marín, C. E. Nanayakkara, J. F. Veyan, B. Warot-Fonrose, S. Joulie, A. Esteìve, C. Tenailleau, Y. J. Chabal, C. Rossi, *ACS Appl. Mater. Interfaces* **2015**, *7*, 11713.
[114] L. Marín, B. Warot-Fonrose, A. Estève, Y. J. Chabal, L. Alfredo Rodriguez, C. Rossi, *ACS Appl. Mater. Interfaces* **2016**, *8*, 13104.
[115] D. Xu, Y. Yang, H. Cheng, Y. Y. Li, K. Zhang, *Combust. Flame* **2012**, *159*, 2202.
[116] Y. Yang, D. Xu, K. Zhang, *J. Mater. Sci*. **2012**, *47*, 1296.
[117] X. Zhou, D. Xu, J. Lu, K. Zhang, *Chem. Eng. J*. **2015**, *266*, 163.
[118] X. Zhou, D. Xu, G. Yang, Q. Zhang, J. Shen, J. Lu, K. Zhang, *ACS Appl. Mater. Interfaces* **2014**, *6*, 10497.
[119] E. L. Dreizin, M. Schoenitz, E. L. Dreizin, M. Schoenitz, *J. Mater. Sci*. **2017**, *52*, 11789.
[120] E. L. Dreizin, M. Schoenitz, In *Metal Nanopowders*, Wiley-VCH Verlag GmbH Co. KGaA, Weinheim, Germany **2014**; p 227.
[121] C. Suryanarayana, *Prog. Mater. Sci*. **2001**, *46*, 1.
[122] C. Suryanarayana, *Rev. Adv. Mater. Sci*. **2008**, *18*, 203.
[123] A. Y. Dolgoborodov, *Combust. Explos. Shock Waves* **2015**, *51*, 86.
[124] A. N. Sterletskii, A. Y. Dolgoborodov, I. V. Kolbanev, M. N. Makhov, S. F. Lomaeva, A. B. Borunova, V. E. Fortov, *Colloid J*. **2009**, *71*, 852.
[125] A. N. Streletskii, I. V. Kolbanev, A. V. Leonov, A. Y. Dolgoborodov, G. A. Vorob'eva, M. V. Sivak, D. G. Permenov, *Colloid J*. **2015**, *77*, 213.

 © 2017 WILEY-VCH Verlag GmbH & Co. KGaA, Weinheim

[126] D. Stamatis, X. Zhu, M. Schoenitz, E. L. Dreizin, P. Redner, *Powder Technol*. **2011**, *208*, 637.
[127] K. Komvopoulos, *Mechanical Testing of Engineering Materials*: 2nd. Ed. Cognella, Incorporated, San Diego, CA **2016**.
[128] D. Stamatis, X. Zhu, A. Ermoline, M. Schoenitz, E. L. Dreizin, P. Redner, *Consolidation of Reactive Nanocomposite Powders*, 45th American Institute of Aeronautics and Astronautics, Denver, CO **2009**.
[129] W. G. Proud, D. M. Williamson, J. E. Field, S. M. Walley, *Chem. Cent. J*. **2015**, *9:52* DOI 10.1186/s13065-015-0128-x.
[130] B. A. Gama, S. L. Lopatnikov, J. W. Gillespie Jr, *Appl. Mech. Rev.* **2004**, *57*, 223.
[131] B. Feng, X. Fang, H. X. Wang, W. Dong, Y. C. Li, *Polymers* **2016**, *8*, 356.
[132] S. Xu, S. Yang, P. Zhao, J. Li, F. Lu, *Lixue Xuebao/Chin. J. Theor. Appl. Mech*. **2009**, *41*, 708.
[133] X. F. Zhang, J. Zhang, L. Qiao, A. S. Shi, Y. G. Zhang, Y. He, Z. W. Guan, *Mater. Sci. Eng. A* **2013**, *581* (Copyright (C) 2015 American Chemical Society (ACS). All Rights Reserved.), 48.
[134] P. D. Zhao, F. Y. Lu, J. L. Li, R. Chen, S. L. Xu, S. Q. Yang, *Hanneng Cailiao/Chin. J. Energ. Mater.* **2009**, *17*, 459.
[135] P. -D. Zhao, F. -Y. Lu, J. -L. Li, R. Chen, S. L. Xu, S. -Q. Yang, *Hanneng Cailiao* **2009**, *17*, 459.
[136] J. E. Field, S. M. Walley, W. G. Proud, H. T. Goldrein, C. R. Siviour, *Int. J. Impact Eng*. **2004**, *30*, 725.
[137] E. P. Fahrenthold, C. H. Yew, *Int. J. Impact Eng*. **1995**, *17*, 303.
[138] B. O'Toole, M. Trabia, R. Hixson, S. K. Roy, M. Pena, S. Becker, E. Daykin, E. MacHorro, R. Jennings, M. Matthes, B. O'Toole, M. Trabia, R. Hixson, S. K. Roy, M. Pena, S. Becker, E. Daykin, E. MacHorro, R. Jennings, M. Matthes, *Procedia Eng*. **2015**, *103*, p 458.
[139] M. Martin S. Hanagud, N. N. *Mater. Sci. Eng. A* **2007**, *443*, 209.
[140] J. L. Breidenich, J. Turner, G. Kennedy, N. N. *J. Phys.: Conf. Series* **2014**, *500* (PART 18) 182006.
[141] M. Gonzales, A. Gurumurthy, G. B. Kennedy, A. M. Gokhale, N. N. Thadhani, *J. Phys.: Conf. Series* **2014**, *500* (PART 5) 052013.
[142] Q. An, S. V. Zybin, W. A. Goddard, A. Jaramillo-Botero, M. Blanco, S. N. Luo, *Phys. Rev. B — Condens. Matter Mater. Phys*. **2011**, *84*, 220101.
[143] T. L. Jackson, D. E. Hooks, J. Buckmaster, *Propellants Explos. Pyrotechn*. **2011**, *36*, 252.
[144] R. Menikoff, *Shock Waves* **2011**, *21*, 141.
[145] S. You, M. W. Chen, D. D. Dlott, K. S. Suslick, *Nat. Commun*. **2015**, *6*, 6581, https://doi.org/10.1038/ncomms7581
[146] J. E. Field, *Acc. Chem. Res*. **1992**, *25*, 489.
[147] X. J. Gu, D. R. Emerson, D. Bradley, *Combust. Flame* **2003**, *133*, 63.
[148] C. M. Tarver, S. K. Chidester, A. L. Nichols Iii, *J. Phys. Chem*. **1996**, *100*, 5794.
[149] E. L. Dreizin, M. Schoenitz, *Prog. Energy Combust. Sci*. **2015**, *50*, 81.
[150] S. Vyazovkin, A. K. Burnham, J. M. Criado, L. A. Pérez-Maqueda, C. Popescu, N. Sbirrazzuoli, *Thermochimica Acta* **2011**, *520*, 1.
[151] S. Vyazovkin, K. Chrissafis, M. L. Di Lorenzo, N. Koga, M. Pijolat, B. Roduit, N. Sbirrazzuoli, J. J. Suñol, *Thermochimica Acta* **2014**, *590*, 1.
[152] E. L. Dreizin, *Prog. Energy Combust. Sci*. **2009**, *35*, 141.
[153] P. Swaminathan, M. D. Grapes, K. Woll, S. C. Barron, D. A. Lavan, T. P. Weihs, *J. Appl. Phys*. **2013**, *113,* 143509, https://doi.org/10.1063/1.4799628
[154] T. S. Ward, M. A. Trunov, M. Schoenitz, E. L. Dreizin, *Int. J. Heat Mass Transfer* **2006**, *49*, 49 43.
[155] R. J. Jacob, D. L. Ortiz-Montalvo, K. R. Overdeep, T. P. Weihs, M. R. Zachariah, *J. Appl. Phys*. **2017**, *121*, 054307.
[156] G. Jian, S. Chowdhury, J. Feng, M. R. Zachariah, In *The Ignition and Combustion Study of Nano-Al and Iodine Pentoxide Thermite*, Combustion Institute, Western States Section Park City, UT **2013**; p 1287.
[157] A. Abraham, S. Zhang, Y. Aly, M. Schoenitz, E. L. Dreizin, *Adv. Eng. Mater.* **2014**. *16*, 909.
[158] Y. Aly, M. Schoenitz, E. L. Dreizin, *Combust. Sci. Technol*. **2011**, *183*, 1107.
[159] S. M. Umbrajkar, S. Seshadri, M. Schoenitz, V. K. Hoffmann, E. L. Dreizin, *J. Propul. Power* **2008**, *24*, 192.
[160] R. A. Williams, J. V. Patel, A. Ermoline, M. Schoenitz, E. L. Dreizin, *Combust. Flame* **2013**, *160*, 734.
[161] S. M. Umbrajkar, M. Schoenitz, E. L. Dreizin, In *Heterogeneous Processes Leading to Metal Ignition in Reactive Nanocomposite Materials*, Reno, NV, AIAA **2007**; p 3582.
[162] Y. L. Shoshin, M. A. Trunov, X. Zhu, M. Schoenitz, E. L. Dreizin, *Combust. Flame* **2006**, *144*, 688.
[163] G. C. Egan, E. J. Mily, J. P. Maria, M. R. Zachariah, *J. Phys. Chem. C* **2015**, *119*, 20401.
[164] G. Young, R. Jacob, M. R. Zachariah, *Combust. Sci. Technol*. **2015**, *187*, 1335.
[165] G. Young, G. Jian, R. Jacob, M. R. Zachariah, *Combust. Sci. Technol*. **2015**, *187*, 1182.
[166] W. Zhou, J. B. DeLisio, X. Wang, G. C. Egan, M. R. Zachariah, *J. Appl. Phys*. **2015**, *118* 114303.
[167] G. Young, N. Piekiel, S. Chowdhury, M. R. Zachariah, *Combust. Sci. Technol*. **2010**, *182*, 1341.
[168] G. Jian, S. Chowdhury, K. Sullivan, M. R. Zachariah, *Combust. Flame* **2013**, *160*, 432.
[169] B. J. Henz, T. Hawa, M. R. Zachariah, *J. Appl. Phys*. **2010**, *107*, 024901.
[170] L. Zhou, N. Piekiel, S. Chowdhury, D. Lee, M. R. Zachariah, *J. Appl. Phys*. **2009**, *106*, 083306.
[171] L. Zhou, N. Piekiel, S. Chowdhury, M. R. Zachariah, *J. Phys. Chem. C* **2010**, *114*, 14269.
[172] S. Mohan, M. A. Trunov, E. L. Dreizin, *J. Propul. Power* **2008**, *24*, 199.
[173] Y. Aly, E. L. Dreizin, *Combust. Flame* **2015**, *162*, 1440.
[174] D. Stamatis, E. L. Dreizin, K. Higa, *J. Propul. Power* **2011**, *27*, 1079.
[175] E. Beloni, E. L. Dreizin, *Combust. Theory Model*. **2012**, *16*, 976.
[176] I. Monk, R. Williams, X. Liu, E. L. Dreizin, *Combust. Sci. Technol*. **2015**, *187*, 1276.
[177] R. A. Williams, J. V. Patel, E. L. Dreizin, *J. Propul. Power* **2014**, *30*, 765.
[178] W. L. Shaw, D. D. Dlott, R. A. Williams, E. L. Dreizin, *Propellants Explos. Pyrotechn*. **2014**, *39*, 444.
[179] I. Monk, M. Schoenitz, E. L. Dreizin, *J. Energetic Mater.* **2017**, *35*, 29.
[180] Y. Yang, S. Wang, Z. Sun, D. D. Dlott, *Propellants Explos. Pyrotech*. **2005**, *30*, 171.
[181] Y. Yang, S. Wang, Z. Sun, D. D. Dlott, *Appl. Phys. Lett*. **2004**, *85*, 1493.
[182] Y. Yang, S. Wang, Z. Sun, D. D. Dlott, *J. Appl. Phys*. **2004**, *95*, 3667.
[183] M. A. Zamkov, R. W. Conner, D. D. Dlott, *J. Phys. Chem. C* **2007**, *111*, 10278.
[184] R. W. Conner, D. D. Dlott, *J. Phys. Chem. A* **2010**, *114*, 6731.
[185] A. Plummer, V. A. Kuznetsov, J. Gascooke, J. Shapter, N. H. Voelcker, *J. Appl. Phys*. **2014**, *116*, 054912.
[186] X. Zheng, A. D. Curtis, W. L. Shaw, D. D. Dlott, *J. Phys. Chem. C* **2013**, *117*, 4866.
[187] K. E. Brown, W. L. Shaw, X. X. Zheng, D. D. Dlott, *Rev Sci Instrum*. **2012**, *83*, 103901.
[188] J. Wang, W. P. Bassett, D. D. Dlott, *J. Appl. Phys*. **2017**, *121*, 085902.
[189] C. M. Berg, D. D. Dlott, *J. Phys.: Conf. Series* **2014**, *500* (PART 14).
[190] G. C. Egan, T. Lagrange, M. R. Zachariah, *J. Phys. Chem. C* **2015**, *119*, 2792.
[191] M. D. Grapes, T. LaGrange, K. Woll, B. W. Reed, G. H. Campbell, D. A. LaVan, T. P. Weihs, *APL Mater.* **2014**, 2 (Copyright (C) 2014

 © 2017 WILEY-VCH Verlag GmbH & Co. KGaA, Weinheim

American Chemical Society (ACS). All Rights Reserved.), 116102/1-116102/7.
[192] J. C. Trenkle, L. J. Koerner, M. W. Tate, N. Walker, S. M. Gruner, T. P. Weihs, T. C. Hufnagel, *J. Appl. Phys*. **2010**, *107*, 113511.
[193] Y. Aly, M. Schoenitz, E. L. Dreizin, *Combust. Flame* **2013**, *160*, 835.
[194] S. Wang, X. Liu, M. Schoenitz, E. L. Dreizin, *Propellants Explos. Pyrotech*. **2017**, *42*, 284.
[195] X. Liu, M. Schoenitz, E. L. Dreizin, *Chem. Eng. J*. **2017**, *325*, 495.
[196] S. Wang, A. Abraham, Z. Zhong, M. Schoenitz, E. L. Dreizin, *Chem. Eng. J*. **2016**, *293*, 112.
[197] R. J. Jacob, B. Wei, M. R. Zachariah, *Combust. Flame* **2016**, *167*, 472.
[198] T. Bazyn, P. Lynch, H. Krier, N. Glumac, *Propellants Explos., Pyrotech*. **2010**, *35*, 93.
[199] T. Bazyn, N. Glumac, H. Krier, T. S. Ward, M. Schoenitz, E. L. Dreizin, *Combust. Sci. Technol*. **2007**, *179*, 457.
[200] B. Aaron Mason, L. J. Groven, S. F. Son, R. A. Yetter, *J. Propul. Power* **2013**, *29*, 1435.
[201] S. F. Son, B. W. Asay, T. J. Foley, R. A. Yetter, M. H. Wu, G. A. Risha, *J. Propul. Power* **2007**, *23*, 715.
[202] V. K. Patel, J. R. Saurav, K. Gangopadhyay, S. Gangopadhyay, S. Bhattacharya, *RSC Adv.* **2015**, *5*, 21471.
[203] S. W. Dean, M. L. Pantoya, A. E. Gash, S. C. Stacy, L. J. Hope-Weeks, *J. Heat Transfer* **2010**, *132*.
[204] J. M. Densmore, K. T. Sullivan, A. E. Gash, J. D. Kuntz, *Propellants Explos. Pyrotech*. **2014**, *39*, 416.
[205] K. T. Sullivan, O. Cervantes, J. M. Densmore, J. D. Kuntz, A. E. Gash, J. D. Molitoris, *Propellants Explos. Pyrotech*. **2015**, *40*, 394.
[206] I. Monk, M. Schoenitz, R. J. Jacob, E. L. Dreizin, M. R. Zachariah, *Combust. Sci. Technol*. **2017**, *189*, 555.
[207] Y. Aly, V. K. Hoffman, M. Schoenitz, E. L. Dreizin, *J. Propul. Power* **2014**, *30*, 96.
[208] A. Abraham, Z. Zhong, R. Liu, S. A. Grinshpun, M. Yermakov, R. Indugula, M. Schoenitz, E. L. Dreizin, *Combust. Sci. Technol*. **2016**, *188*, 1345.
[209] S. A. Grinshpun, M. Yermakov, R. Indugula, A. Abraham, M. Schoenitz, E. L. Dreizin, *Aerosol Sci. Technol*. **2017**, *51*, 224.
[210] E. M. Hunt, M. L. Pantoya, *Intermetallics* **2010**, *18*, 1612.
[211] B. Asay, B. Henson, P. Dickson, C. Fugard, D. Funk, *AIP Conf. Proc*. AIP: Vol. *429*, **1998**; p 567.
[212] M. T. Beason, I. E. Gunduz, S. F. Son, *Acta Mater.* **2017**, *133*, 247.
[213] B. A. Mason, L. J. Groven, S. F. Son, *J. Appl. Phys. (Melville, NY, U. S.)* **2013**, *114* (Copyright (C) 2014 American Chemical Society (ACS). All Rights Reserved.), 113501/1-113501/7. https://doi.org/10.1063/1.4821236
[214] R. V. Reeves, A. S. Mukasyan, S. F. Son, *J. Phys. Chem. C* **2010**, *114*, 14772.
[215] B. B. Aydelotte, N. N. Thadhani, *Mater. Sci. Eng. A* **2013**, *570*, 164.
[216] R. G. Ames, In *Vented Chamber Calorimetry for Impact-Initiated Energetic Materials*, 43rd AIAA Aerospace Sciences Meeting and Exhibit – Meeting Papers, **2005**; p 15391.
[217] R. G. Ames, *Mater. Res. Soc. Symp. Proc*. **2006**; p 123.
[218] B. Sorensen, *Procedia Eng*. **2015**, *218*, 569.
[219] B. Feng, X. Fang, Y. C. Li, S. Z. Wu, Y. M. Mao, H. X. Wang, *Cent. Eur. J. Energetic Mater.* **2016**, *13*, 989.
[220] Y. Li, C. Jiang, Z. Wang, P. Luo, *Materials* **2016**, *9*, 936. https://doi.org/10.3390/ma9110936
[221] C. Ge, Y. Dong, W. Maimaitituersun, Y. Ren, S. Feng, *Propellants Explos. Pyrotech*. **2017**, *42*, 514.
[222] Y. Li, Z. Wang, C. Jiang, H. Niu, *Materials* **2017**, *10*, 175. https://doi.org/10.3390/ma10020175
[223] F. Y. Xu, Y. F. Zheng, Q. B. Yu, X. P. Zhang, H. F. Wang, *Int. J. Impact Eng*. **2017**, *104*, 38.
[224] X. F. Zhang, A. S. Shi, L. Qiao, J. Zhang, Y. G. Zhang, Z. W. Guan, *J. Appl. Phys. (Melville, NY, U. S.)* **2013**, *113*, 173513. https://doi.org/10.1063/1.4803712
[225] J. Zhou, Y. He, Y. He, C. T. Wang, *Propellants Explos. Pyrotech*. **2017**, *42*, 603.
[226] A. Y. Dolgoborodov, M. N. Makhov, I. V. Kolbanev, A. N. Streletskiĭ, V. E. Fortov, *JETP Lett*. **2005**, *81*, 311.
[227] D. L. Gur'ev, Y. A. Gordopolov, S. S. Batsanov, A. G. Merzhanov, V. E. Fortov, *Appl. Phys. Lett*. **2006**, *88*, 1.
[228] J. H. S. Lee, S. Goroshin, A. Yoshinaka, M. Romano, J. Jiang, I. Hooton, F. Zhang, J. H. S. Lee, S. Goroshin, A. Yoshinaka, M. Romano, J. Jiang, I. Hooton, F. Zhang, Attempts to initiate detonations in metal-sulphur mixtures. In *Shock Compression of Condensed Matter – 1999: Proceedings of the Conference of the American Physical Society Topical Group on Shock Compression of Condensed Matter held at Snowbird, Utah, June 27-July 2, 1999*, M. D. Furnish, L. C. Chhabildas, R. S. Hixson, Eds. American Inst. of Physics: **2000**; p 775.
[229] F. X. Jetté, S. Goroshin, A. J. Higgins, J. J. Lee, *Combust. Explos. Shock Waves* **2009**, *45*, 211.
[230] F. X. Jetté, A. J. Higgins, S. Goroshin, D. L. Frost, Y. Charron-Tousignant, M. I. Radulescu, J. J. Lee, *J. Appl. Phys*. **2011**, *109*, 084905.
[231] F. X. Jetté, S. Goroshin, D. L. Frost, A. J. Higgins, J. J. Lee, *Propellants Explos. Pyrotech*. **2012**, *37*, 345.
[232] P. H. Chiu, K. L. Olney, A. Higgins, M. Serge, D. J. Benson, V. F. Nesterenko, *Appl. Phys. Lett*. **2013**, *102*, 241912.
[233] K. L. Olney, P. H. Chiu, A. Higgins, M. Serge, T. P. Weihs, G. M. Fritz, A. K. Stover, D. J. Benson, V. F. Nesterenko, *Philos. Mag.* **2014**, *94*, 3017.
[234] J. Guadarrama, E. L. Dreizin, N. Glumac, *Propellants Explos. Pyrotech*. **2016**, *41*, 605.
[235] D. L. Frost, J. Loiseau, S. Goroshin, F. Zhang, A. Milne, A. Longbottom, *AIP Conf. Proc. 1793*, 120019, **2017**.

 © 2017 WILEY-VCH Verlag GmbH & Co. KGaA, Weinheim